iScience

CellPress
OPEN ACCESS

Article

Aβ*56 is a stable oligomer that impairs memory function in mice

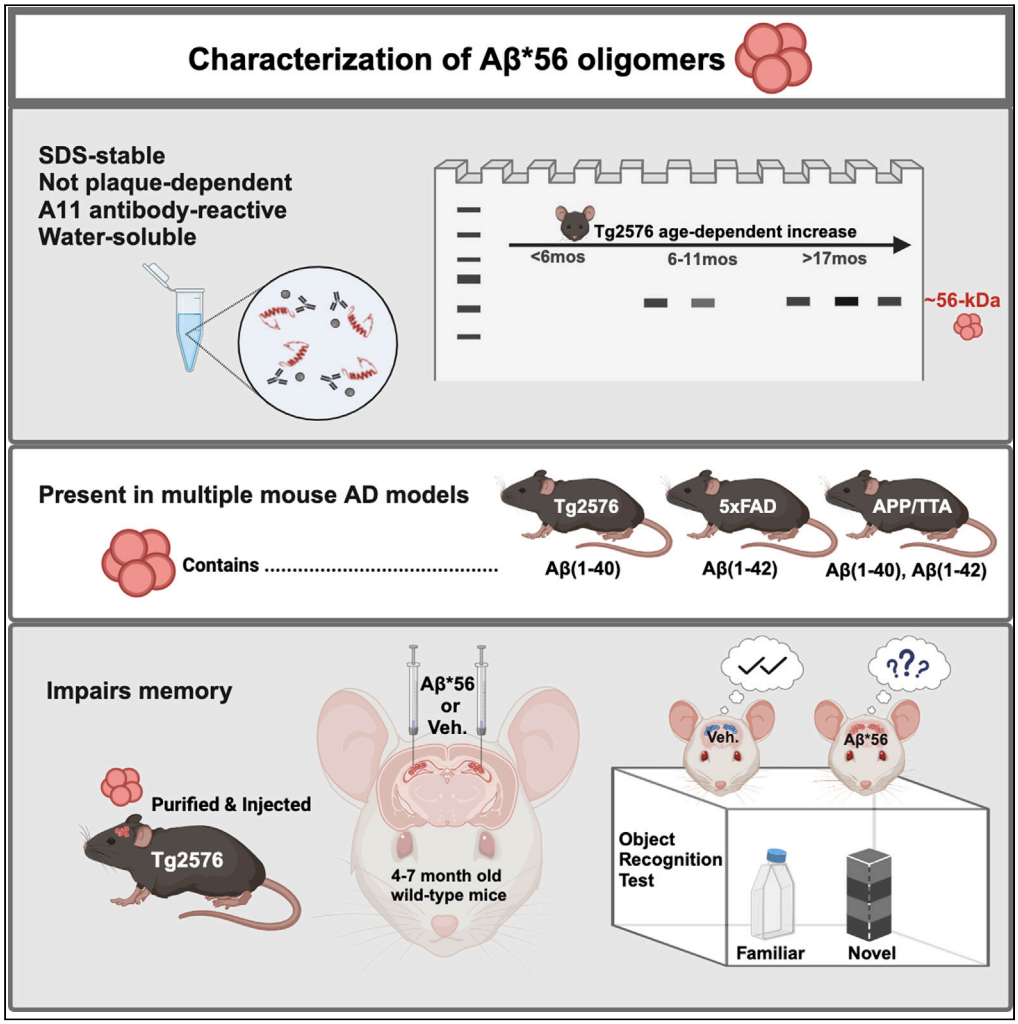

Peng Liu, Ian P. Lapcinski, Chris J.W. Hlynialuk, ..., Samantha L. Shapiro, Lisa J. Kemper, Karen H. Ashe

liuxx726@umn.edu (P.L.)
hsiao005@umn.edu (K.H.A.)

Highlights

Aβ*56 is a ~56-kDa, SDS-stable, A11-reactive, water-soluble, brain-derived oligomer

Aβ*56 is produced in multiple transgenic Alzheimer mouse models

Aβ*56 contains canonical Aβ and forms before dense-core, neuritic plaques appear

Purified Aβ*56 from mice modeling Alzheimer disease impairs memory of young, healthy wild-type mice

Liu et al., iScience 27, 109239
March 15, 2024
https://doi.org/10.1016/j.isci.2024.109239

iScience

CellPress
OPEN ACCESS

Article

Aβ*56 is a stable oligomer that impairs memory function in mice

Peng Liu,[1,2,*] Ian P. Lapcinski,[1,2] Chris J.W. Hlynialuk,[1,2] Elizabeth L. Steuer,[1,2] Thomas J. Loude, Jr.,[1,2] Samantha L. Shapiro,[1,2] Lisa J. Kemper,[1,2] and Karen H. Ashe[1,2,3,*]

SUMMARY

Amyloid-β (Aβ) oligomers consist of fibrillar and non-fibrillar soluble assemblies of the Aβ peptide. Aβ*56 is a non-fibrillar Aβ assembly that is linked to memory deficits. Previous studies did not decipher specific forms of Aβ present in Aβ*56. Here, we confirmed the memory-impairing characteristics of Aβ*56 and extended its biochemical characterization. We used anti-Aβ(1-x), anti-Aβ(x-40), anti-Aβ(x-42), and A11 anti-oligomer antibodies in conjunction with western blotting, immunoaffinity purification, and size-exclusion chromatography to probe aqueous brain extracts from Tg2576, 5xFAD, and APP/TTA mice. In Tg2576, Aβ*56 is a ~56-kDa, SDS-stable, A11-reactive, non-plaque-dependent, water-soluble, brain-derived oligomer containing canonical Aβ(1-40). In 5xFAD, Aβ*56 is composed of Aβ(1-42), whereas in APP/TTA, it contains both Aβ(1-40) and Aβ(1-42). When injected into the hippocampus of wild-type mice, Aβ*56 derived from Tg2576 mice impairs memory. The unusual stability of this oligomer renders it an attractive candidate for studying relationships between molecular structure and effects on brain function.

INTRODUCTION

Aβ*56 was the first brain-derived amyloid-β (Aβ) oligomer shown to impair memory in mice and rats.[1] Aβ*56 forms before dense-core, neuritic plaques appear and is found both inside dense-core plaques and dispersed outside in the brain parenchyma.[2] The discovery of Aβ*56 stimulated interest in Aβ oligomers as mediators of cognitive deficits in Alzheimer disease (AD) and spurred the development of new, oligomer-specific, therapeutic antibodies. Aβ*56 is but one of many variants of brain-derived Aβ oligomers. Other brain-derived, oligomeric variants include dimers and trimers,[3] prefibrillar oligomers that bind A11 antibodies,[4] amylospheroids,[5] globulomers,[6] fibrillar oligomers that bind OC antibodies,[7] protofibrillar oligomers that bind mAb158/lecanemab antibodies,[8] intraneuronal oligomers that bind NU-1 anti-Aβ-derived diffusible ligand (ADDL) antibodies,[9] annular protofibrils,[10] amyloid pores,[11] oligomers that bind crenezumab,[12] oligomers that bind aducanumab,[13] oligomers that bind ACU3B3/ACU193 anti-ADDL antibodies,[14] oligomers that bind α-sheets,[15] and oligomers that bind JD1 antibodies,[16] whose structure, spatial distribution, temporal expression, biogenesis, and effects on brain function are topics of active study with important therapeutic implications.

Aβ*56 correlates with aging and impaired memory in mice, dog, and humans. Billings et al. found that repeated behavioral training decreases Aβ*56 levels and amyloid plaque loads and improves memory function, reflecting a possible connection between brain activity and Aβ aggregation.[17] Pop et al. showed a positive correlation between age and Aβ*56 in aqueous extracts of temporal cortex from beagles.[18] Yoo et al. demonstrated an association between Aβ*56 and age-related apoptosis in the ectoturbinate olfactory epithelium of Tg2576[19] mice.[20] Building upon these findings, Yoo et al. investigated nasal fluid in living, elderly human participants and found a ~2.9-fold increase in Aβ*56 levels in individuals diagnosed with AD compared with controls.[21] In addition, over three years, cognitive performances of individuals with Aβ*56 levels above the median value deteriorate, whereas those with levels below the median remain stable.[21]

In several specific lines of amyloid precursor protein (APP) transgenic mice such as Tg2576, hAPP-J20, Arc6, APP/TTA, and rTg9191, memory deficits are more closely associated with Aβ*56 than with dense-core, neuritic plaques. Cheng et al. demonstrated that spatial reference memory in hAPP-J20[22] mice expressing moderate levels of APP with the Swedish (K670N, M671L) and Indiana (V717F) mutations negatively correlates with levels of Aβ*56 but not dense-core plaque loads.[23] Arc6[24] mice, which express low levels of APP with the Swedish, Indiana, and Arctic (E693G) mutations promoting fibril formation leading to plaque loads that are higher than those in hAPP-J20 mice, lack Aβ*56 and, accordingly, exhibit normal spatial reference memory.[23] Meilandt et al. showed that neprilysin overexpression in hAPP-J20 mice reduces amyloid plaques but not Aβ*56 and does not improve spatial reference memory, elevated plus-maze performance, or premature mortality.[25] Liu et al. showed that grape-seed polyphenolic extracts in drinking water, previously shown to attenuate cognitive impairment in Tg2576 mice,[26]

[1]N. Bud Grossman Center for Memory Research and Care, Minneapolis, MN 55455, USA
[2]Department of Neurology, University of Minnesota, Minneapolis, MN 55455, USA
[3]Lead contact
*Correspondence: liuxx726@umn.edu (P.L.), hsiao005@umn.edu (K.H.A.)
https://doi.org/10.1016/j.isci.2024.109239

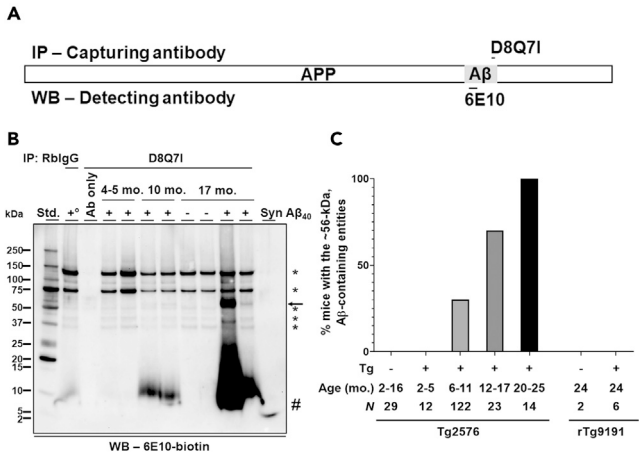

Figure 1. Age-related presence of ~56-kDa, SDS-stable, water-soluble, Aβ-containing entities in Tg2576 mice

(A) A schematic illustration of epitopes of capturing and detecting antibodies used in immunoprecipitation (IP)/western blotting (WB) for (B). Capturing antibody: rabbit monoclonal D8Q7I that is directed against the C-terminus of Aβ(x-40), detecting antibody: biotinylated mouse monoclonal 6E10 that is directed against Aβ(3-8). APP, amyloid precursor protein; Aβ, amyloid-β.

(B) A representative IP/WB analysis showing that D8Q7I-precipitated entities electrophoresed at ~56 kDa (arrow) are detected by biotinylated 6E10 (6E10-biotin) in 10-month-old and 17-month-old Tg2576 (+) mice but not in 4- to 5-month-old Tg2576 (+) mice, in 17-month-old littermates of Tg2576 mice (–), or when no Tg2576 brain extracts were used (Ab only). No ~56-kDa entities are detected when generic rabbit immunoglobulin G (RbIgG) was used to precipitate brain extracts (+°, combined brain extracts of the four 10-month- and 17-month-old Tg2576 mice, each contributing 25% of the total proteins). Ab, capturing antibody D8Q7I. Syn $A\beta_{40}$, synthetic Aβ(1-40) (4 ng), serving as a positive control for WB. #, monomeric Aβ(x-40). *, non-specifically detected entities. kDa, kilo-Daltons. Std., protein standards; and mo., months.

(C) The percentage of Tg2576 mice expressing ~56-kDa entities increases with age. Non-transgenic littermates (–) of Tg2576 and rTg9191 mice, 2- to –5-month-old Tg2576 mice (+), and 24-month-old rTg9191 mice (+) do not express the ~56-kDa entity. The ages (mo., months) shown in the figure are defined as follows: 2–16 months, 1.5–16.4 months; 2–5 months, 1.5–5.4 months; 6–11 months, 5.5–11.4 months; 12–17 months, 11.5–17.4 months; 20–25 months, 19.5–25.4 months; and 24 months, 23.5–24.4 months. The total number (*N*) of mice of each age group is listed. Detailed information for the calculation is listed in Table S1. See also Figures S1, S2, S30, and S34; Tables S1, S2, and S3.

reduce levels of Aβ*56 by 48% but do not change levels of Aβ dimers.[27] Castillo-Carran et al. reported improved performance in contextual fear conditioning and novel object recognition in Tg2576 mice two weeks after a single intravenous injection of tau-oligomer monoclonal antibodies is accompanied by ~60% reduction in Aβ*56 level and ~1.8-fold increase in Thioflavin S (ThioS) amyloid plaque load,[28] suggesting that tau oligomers promote off-pathway non-fibril and depress on-pathway fibril aggregation of Aβ. Fowler et al. discovered that reducing Aβ production in APP/TTA mice lowers Aβ*56 levels and improves performance in spatial reference memory without changing ThioS amyloid plaque loads.[29] Liu et al. furnished a rationale for the dissociation between dense-core amyloid plaques and impaired cognition by demonstrating that Aβ dimers, which are confined to dense-core plaques in Tg2576 and rTg9191 mice,[30] do not impair memory function unless they are extracted from the plaques and dispersed in the brain.[2,30]

Here, we confirm and extend the characterization of Aβ*56. We show that it is a ~56-kDa, A11-reactive, SDS-stable, non-plaque-dependent, water-soluble, brain-derived oligomer that contains canonical Aβ(1-40) and/or Aβ(1-42) and impairs memory function when injected into young, healthy mice.

RESULTS

Age-related appearance of a ~56-kDa, SDS-stable, water-soluble, Aβ-containing entity in Tg2576 mice

We captured proteins in aqueous brain extracts by immunoprecipitation (IP) with D8Q7I antibodies recognizing the C-terminus of Aβ(x-40), fractionated captured proteins by sodium dodecyl sulfate (SDS)-polyacrylamide gel electrophoresis (PAGE), transferred proteins to nitrocellulose membranes, and probed them using biotinylated 6E10 antibodies recognizing Aβ(3-8) (Figure 1A). We screened both neuritic-plaque-free (≤12 months of age)[31] and neuritic-plaque-bearing (≥13 months of age)[31] Tg2576 mice and found a ~56-kDa, 6E10-reactive entity in a subset of Tg2576 mice, but not in their age-matched, non-transgenic littermates or aged rTg9191 mice (Figures 1B and S1–S27; Table S1). We detected no other specific 6E10-reactive entities besides the ~56-kDa entity and ~4.5-kDa monomeric Aβ.

The ~56-kDa, 6E10-reactive entity was present in 0% of 2- to 5-month-old, 30% of 6- to 11-month-old, 70% of 12- to 17-month-old, and 100% of 20- to 25-month-old Tg2576 mice but not in 24-month-old rTg9191 mice (Figures 1C and S1–S27; Table S1). Levels of the ~56-kDa entity increased with age ($p = 0.0006$, Kruskal-Wallis test); its levels were 3.6-fold (group median) higher in 20- to 25-month than 6- to 11-month-old mice ($p = 0.0011$, *post-hoc* Dunn's multiple comparison test) and 2.5-fold (group median) higher in 20- to 25-month-old than 12- to 17-month-old mice ($p = 0.0133$, *post-hoc* Dunn's multiple comparison test) (Figure S28). In addition, levels of the ~56-kDa entity correlated with levels of Aβ monomers ($\rho = 0.7731$, $p < 0.0001$, Spearman correlation) (Figure S29). Of note, there was

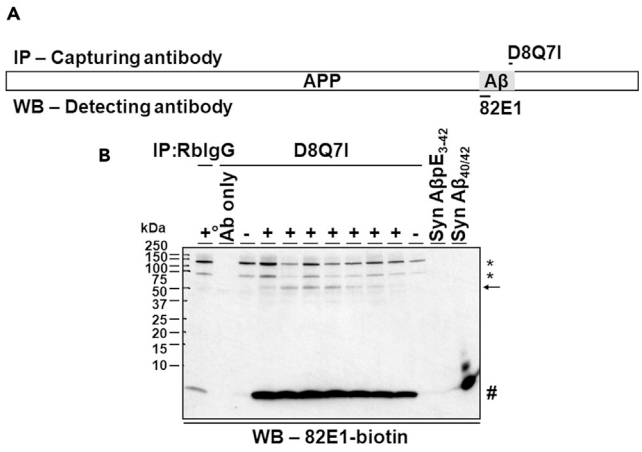

Figure 2. Canonical Aβ(1-40) is present in the ~56-kDa, SDS-stable, water-soluble, Aβ-containing entities in Tg2576 mice

(A) A schematic illustration of epitopes of capturing and detecting antibodies used in immunoprecipitation (IP)/western blotting (WB) for (B). Capturing antibody: rabbit monoclonal D8Q7I; detecting antibody: biotinylated mouse monoclonal 82E1 that is directed against the N-terminus of Aβ(1-x). APP, amyloid precursor protein; Aβ, amyloid-β.

(B) A representative IP/WB analysis showing that D8Q7I-precipitated entities electrophoresed at ~56 kDa (arrow) are detected by biotinylated 82E1 (82E1-biotin) in 8- to 12-month-old Tg2576 mice (+) but not in age-matched, non-transgenic littermates (–). No ~56-kDa, D8Q7I-precipitated entities are detected when no Tg2576 brain extracts were used (Ab only). No ~56-kDa entities are detected in Tg2576 mice when generic rabbit immunoglobulin G (RbIgG) was used to precipitate brain extracts (+°, combined brain extracts of the seven Tg2576 mice, each contributing 14.3% of the total proteins). Ab, capturing antibody D8Q7I. Syn AβpE3-42, synthetic $Aβ_{42}$ with the 3rd amino acid being a pyroglutamate (30 ng), serving as a negative control for WB, and Syn $Aβ_{40/42}$, synthetic Aβ(1-40) (5 ng) and Aβ(1-42) (5 ng), serving as a positive control for WB. #, monomeric Aβ; $, dimeric Syn $Aβ_{40/42}$; @, trimeric Syn $Aβ_{40/42}$; and *, non-specifically detected entities. kDa, kilo-Daltons. See also Figures S31–S33 and S40; Tables S1, S2, and S3.

no significant difference in the prevalence of the ~56-kDa entity between male (39% [27/70]) and female (40% [40/101]) Tg2576 mice between 2 and 25 months of age; further, there was no significant difference in levels of the ~56-kDa entity between male and female Tg2576 mice of 7–25 months of age (U = 118, p = 0.2711, two-tailed Mann-Whitney U test) (Figure S30).

Canonical Aβ(1-40) is present in the ~56-kDa, SDS-stable, water-soluble, Aβ-containing entities

To define the N-terminus of the 6E10-reactive ~56 kDa entities, we captured proteins in aqueous brain extracts by IP with D8Q7I antibodies recognizing the C-terminus of Aβ(x-40), fractionated captured proteins by SDS-PAGE, transferred proteins to nitrocellulose membranes, and probed them using biotinylated 82E1 antibodies recognizing the N-terminus of Aβ(1-x) (Figure 2A). Immunoprecipitated proteins probed with 82E1 antibodies revealed a ~56-kDa entity and monomeric Aβ in 8- to 12-month-old, neuritic-plaque-free, Tg2576 mice but not in non-transgenic littermates (Figure 2B). Using the same methodology, we also found ~56-kDa entities containing canonical Aβ(1-40) in 14- to 21-month, neuritic-plaque-bearing Tg2576 mice (Figure S31). We concluded that the ~56-kDa, SDS-stable, water-soluble entities in Tg2576 mice contain canonical Aβ(1-40).

To determine the prevalence of mice harboring the ~56-kDa entity that contained Aβ(1-40), 92% of 2- to 5-month-old (6 males and 5 females), 45% of 6- to 11-month-old (26 males and 29 females), 25% of 12- to 17-month-old (4 males and 2 females), and 36% of 20- to 25-month-old (3 males and 2 females) Tg2576 mice listed in Table S1 were sampled, D8Q7I-precipitated entities were probed using biotinylated 82E1, and the presence of the ~56-kDa, 82E1-reactive entity in these sampled mice was similarly determined. We discovered that mice harboring the ~56-kDa, 6E10-reactive entities (Figures 1B and 1C) also showed the presence of ~56-kDa entities responsive to the 82E1 antibody; conversely, mice lacking ~56-kDa, 6E10-reactive entities did not exhibit any ~56-kDa entities binding to the 82E1 antibody (data not shown). These findings indicate that the prevalence of the 82E1-reactive entities at each age period is identical to that of the 6E10-reactive entities.

Next, we reversed the order of the antibodies used for IP and western blotting. Proteins immunoprecipitated with 82E1 antibodies that were probed on western blots with D8Q7I antibodies did not reveal ~56-kDa assemblies (Figure S32), suggesting that the free N-terminus is inaccessible under non-denaturing conditions.

Some forms of Aβ aggregate to form amyloid fibrils more readily than Aβ(1-40), notably Aβ(x-42).[32] We sought, therefore, to determine whether the ~56-kDa entity contains Aβ(x-42). We captured proteins in brain extracts of neuritic-plaque-free Tg2576 mice that contained the ~56-kDa entity using D3E10 antibodies recognizing Aβ(x-42) and analyzed the captured proteins in western blots probed with biotinylated 82E1 antibodies. We detected no ~56-kDa bands in these specimens (Figure S33A). We confirmed these results using Aβ(x-40) and Aβ(x-42) antibodies from another source (Figure S34). We also reversed the order of the antibodies used for IP and western blotting. We found no ~56-kDa entities in 82E1-precipitated proteins when they were probed on western blots with D3E10 antibodies (Figures S33B and S33C). These studies indicate that, within the limits of our assay, the ~56-kDa, Aβ-containing entity in neuritic-plaque-free Tg2576 mice contains no detectable Aβ(x-42).

The ~56-kDa, Aβ(1-40)-containing entities are not artificially formed by exposure to SDS

Although our results indicate that the ~56-kDa entities contain canonical Aβ(1-40), these data do not exclude the possibility that they are artificially generated from monomers exposed to SDS. It is also possible that they are not oligomers, but rather complexes of Aβ(1-40) monomers covalently bound together or to other macromolecules.

To investigate the possibility that the ~56-kDa, Aβ(1-40)-containing entity may be artificially generated from monomers exposed to SDS, we used non-denaturing size-exclusion chromatography (SEC) to fractionate aqueous brain extracts from 10- to 11-month-old pre-neuritic-plaque Tg2576 mice and examined every other eluted fractions by SDS-PAGE and western blotting with biotinylated 82E1 and D8Q7I antibodies (Figure 3). Numerous non-specific bands represent non-specific binding to the secondary detection agent NeutrAvidin (Figure S35).

We found most of the 82E1-reactive, ~56-kDa entities in fractions corresponding to ~46–120 kDa (fractions 59–67) with a peak at ~55 kDa, but not in the fractions containing monomeric Aβ, which appeared in fractions corresponding to ~160 to >2,000 kDa and ~10–24 kDa (fractions 37–57 and 75–81, respectively) (Figures 3A and 3B). We observed the same pattern in extracts from younger, 7- to 9-month-old mice (Figure S36). The early peak of monomers reflects the presence of large aggregates containing weakly associated monomers, whereas the late peak contains small, SDS-sensitive assemblies, findings that are consistent with a previously published result.[33] A minor portion of the ~56-kDa entities were found in fractions corresponding to ~200–540 kDa (fractions 47–55) with a peak at ~290 kDa. Similar results were found for the younger mice, except there were fewer monomers in the later fractions (Figure S36). The presence of the ~56-kDa entity in fractions corresponding to higher molecular masses suggests that under non-denaturing conditions, some ~56-kDa entities bind weakly together. A specific, ~14-kDa band appeared in fractions corresponding to ~24–40 kDa (fractions 69–75) with a peak at ~29 kDa.

When probed with D8Q7I antibodies, we found a doublet at ~56 kDa (Figures 3C and 3D). The upper band was present in fractions corresponding to ~32–87 kDa (fractions 60–72) with a peak at ~55 kDa, whereas the lower band was present in fractions corresponding to ~62–335 kDa (fractions 52–62) with a peak at ~180 kDa. The ~56-kDa bands were absent in fractions containing monomeric Aβ, which appeared in fractions corresponding to ~500 to >2,000 kDa and ~17.5–20 kDa (fractions 36–48 and 76–78, respectively). A specific, ~14-kDa band appeared in fractions corresponding to ~26–45 kDa (fractions 68–74) with a peak at ~28 kDa.

To determine whether the presence of neuritic plaques affects the native state of the 82E1-reactive, ~56-kDa entities, we also examined the SEC profile of extracts from old, 15- to 22-month-old Tg2576 mice (Figure S37). We found most of the 82E1-reactive, ~56-kDa entities in fractions corresponding to ~2,400–1,160 kDa (fractions 35–41) with a peak at ~2,000 kDa (fraction 37) and minor peaks at ~1,130 kDa (fraction 43), ~200 kDa (fraction 55), and ~66 kDa (fraction 61). Monomers were detected mainly in fractions corresponding to ~2,400–1,160 kDa (fractions 35–41), with subsequently a sharp decline and no peaks. Although the main peaks of the monomers and ~56-kDa entities overlapped, there were few monomers in the three later ~56-kDa peaks. We interpreted these results to indicate that in old Tg2576 mice, the ~56-kDa entities associated with large aggregates present in neuritic plaques. The low levels of monomers in the subsequent ~56-kDa peaks support our conclusion from pre-neuritic-plaque mice (Figures 3 and S36) that the ~56-kDa entities are not artificially formed from monomers.

These results indicate that a ~56-kDa entity that is not artificially formed from monomers or lower molecular weight Aβ species exists and that its mass is similar whether measured by SEC or SDS-PAGE. The ~14-kDa band may represent a trimeric form of Aβ that weakly binds to another trimer to form higher-*n* oligomers. The constituents in the D8Q7I-reactive, ~56-kDa doublets are unclear; it is possible that they reflect heterogeneity in the N-termini of the constituent Aβ species that assemble to form hetero-oligomers.

The ~56-kDa, Aβ(1-40)-containing entities dissociate in denaturants

To determine whether the ~56-kDa entity is a complex of Aβ(1-40) molecules that are covalently bound to themselves or other macromolecules, we subjected desiccated proteins in aqueous brain extracts to urea, guanidine hydrochloride (GuHCl), and 1,1,1,3,3,3-hexafluoro-2-propanol (HFIP). We resuspended the denatured proteins in Tris-buffered saline (TBS) and analyzed them by IP using D8Q7I antibodies followed by western blotting using 82E1 antibodies. Non-denatured, captured proteins (exposed to TBS only) probed with 82E1 antibodies revealed not only a ~56-kDa band but also bands at ~40 kDa, ~35 kDa, and ~12 kDa, in addition to monomers (Figure 4). All four bands disappeared after the captured proteins were denatured using urea or GuHCl, indicating that the proteins in these bands are not covalently linked (Figure 4). We cannot exclude the possibility that a macromolecule is non-covalently bound to Aβ(1-40) in a manner that resists SDS. Arguing against this possibility is that the ~56-kDa, ~40-kDa, ~35-kDa, and ~12-kDa entities would require Aβ(1-40) to be complexed to a different macromolecule in each band, which seems unlikely. We concluded that the ~56-kDa entity is an SDS-stable, water-soluble, brain-derived oligomer containing canonical Aβ(1-40), also known as Aβ*56.

Isolated Aβ*56 is a stable, A11-reactive, ~56-kDa oligomer containing Aβ(1-40)

To investigate the properties of isolated Aβ*56, we immunopurified Aβ(x-40) species from aqueous brain extracts of 15- to 22-month-old Tg2576 mice using a D8Q7I-immobilized immunoaffinity matrix. We used 82E1 and A11 antibodies to probe immunoblots of Aβ(x-40) species, which were not detectable in the absence of these antibodies (Figure S38). When probed with 82E1 antibodies under denaturing conditions (i.e., immunoprecipitated proteins boiled in β-mercaptoethanol and fractionated by SDS-PAGE), we found bands corresponding to ~56 kDa, between 10 and 50 kDa, and monomers, indicating that these species contain canonical Aβ(1-40) (Figure 5A). These data show that Aβ*56 can exist as a stable complex that resists boiling in β-mercaptoethanol and exposure to SDS.

Next, we probed immunopurified Aβ(x-40) species using polyclonal, anti-oligomer, A11 antibodies. We previously showed that A11 does not recognize anti-parallel or in-register, parallel β-sheets generated from synthetic Aβ and binds entities in neuritic-plaque-free hAPP-J20 and Tg2576 APP transgenic mice.[2] We tested four different batches and found that A11 from two batches detects ~56-kDa

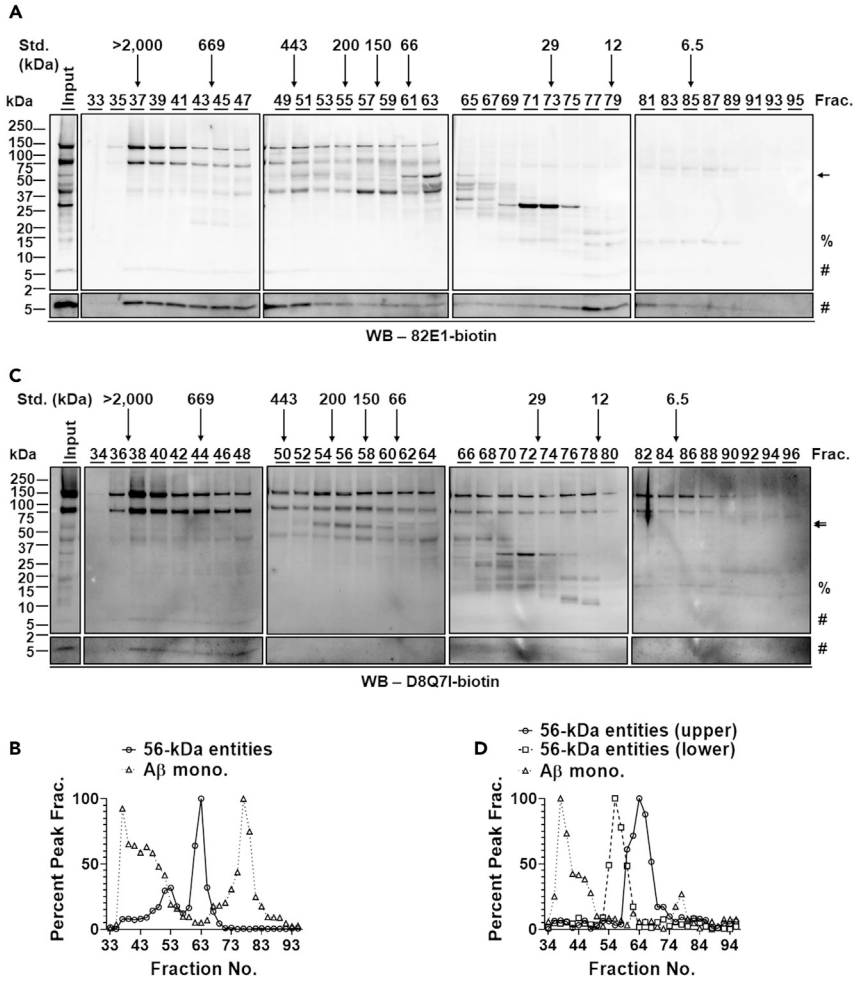

Figure 3. The ~56-kDa, Aβ(1-40)-containing entities are not artificially formed by exposure to SDS

(A) Representative western blotting (WB) analyses showing the detection of the ~56-kDa, Aβ-containing entities (arrow, fractions [Frac.] 47–67), ~14-kDa entities (%, Frac. 69–75), and monomeric Aβ (#, frac. 37–55 and 75–81) in odd-numbered size-exclusion chromatography (SEC) fractions (Frac. 33–95) of 10- to 11-month-old Tg2576 brain extracts using biotinylated 82E1 (82E1-biotin). The four WB images (i.e., Frac. 33–47, 49–63, 65–79, and 81–95) shown were obtained using the same exposure time (20 s), and the WB band patterns and intensities of the input material (2.5% (w/v) of the brain extracts used for SEC) within each of the four WB images are comparable. A WB of the input is shown in the far-left panel. To better visualize monomeric Aβ, WB images at a longer exposure time (100 s) are shown in lower panels. The elution profile of biomolecule standards (Std.) of varied sizes is shown above the WB images. kDa, kilo-Daltons.

(B) Quantitative analyses of levels of the ~56-kDa, 82E1-reactive entities and monomeric Aβ in SEC fractions. The level of the ~56-kDa entities in each fraction is normalized to its highest level in fraction 63 and of monomeric Aβ (Aβ mono.) in each fraction is normalized to its highest level in fraction 77.

(C) Representative WB analyses showing the detection of the ~56-kDa, Aβ-containing entities (arrows, Frac. 52–72), ~14-kDa entities (%, Frac. 68–74), and monomeric Aβ (#, Frac. 36–48 and 76–78) in even-numbered SEC fractions (Frac. 34–96) of 10- to 11-month-old Tg2576 brain extracts using biotinylated D8Q7I (D8Q7I-biotin). The four WB images (i.e., Frac. 34–48, 50–64, 66–80, and 82–96) were obtained using the same exposure time (50 s), and the WB band patterns and intensities of the input material (2.5% [w/v] of the brain extracts used for SEC) within each of the four WB images are comparable. A WB of the input is shown in the far-left panel. To better visualize monomeric Aβ, WB images at a longer exposure time (100 s) are shown in lower panels. The elution profile of biomolecule standards (Std.) of varied sizes is shown above the WB images. kDa, kilo-Daltons.

(D) Quantitative analyses of levels of the ~56-kDa, D8Q7I-reactive entities and monomeric Aβ in SEC fractions. Levels of the ~56-kDa entities in each fraction are normalized to their highest level in fraction 56 (lower band) and fraction 64 (upper band), and the level of monomeric Aβ (Aβ mono.) in each fraction is normalized to its highest level in fraction 38. See also Figures S35–S37; Tables S1, S2, and S3.

entities (Figure S39). We fractionated immunopurified Aβ(x-40) species by SDS-PAGE under denaturing (Figure 5B) or semi-denaturing (i.e., not boiled and no β-mercaptoethanol) (Figure 5C) conditions and found a ~56-kDa, A11-reactive band under both conditions. Under denaturing conditions (Figure 5B), Aβ*56 was the sole A11-reactive species, whereas under semi-denaturing conditions (Figure 5C), there were additional species migrating at ~27 kDa, ~22 kDa, and ~10–15 kDa, which likely represent less stable Aβ(x-40) assemblies.

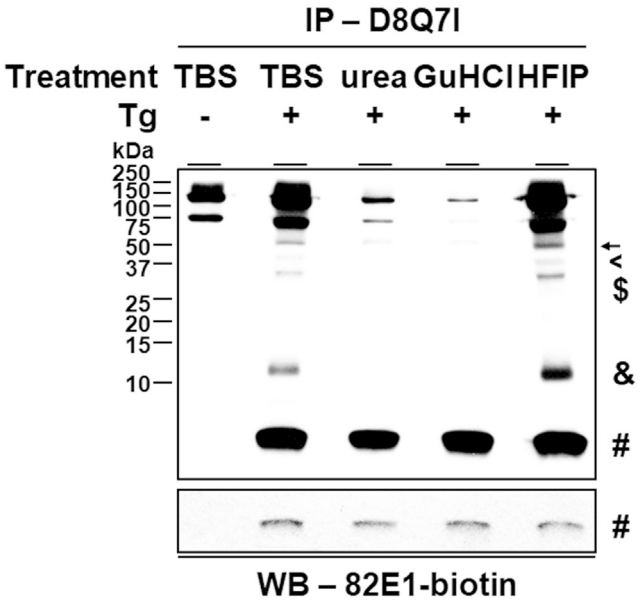

Figure 4. The ~56-kDa, Aβ(1-40)-containing entities are dissociated by denaturants

A representative immunoprecipitation (IP)/western blotting (WB) analysis showing the detection of a set of 82E1-reactive Aβ(1-40)-containing entities—the ~56-kDa (arrow), ~40-kDa (<), ~35-kDa ($), ~12-kDa (&), and monomeric Aβ (#)—in D8Q7I-precipitated brain extracts of 8- to 11-month-old Tg2576 mice (+) but not age-matched littermates (–). The detection of these entities, except for monomeric Aβ, is diminished after treating the D8Q7I-precipitated molecules with either 8M urea or 6M guanidine hydrochloride (GuHCl) but not 100% (v/v) 1,1,1,3,3,3-hexafluoro-2-propanol (HFIP), compared with the samples treated with Tris-buffered saline (TBS). Monomeric Aβ is similarly detected following these different treatments. Upper panel, light exposure; and lower panel, heavy exposure. Tg, transgene expressing human amyloid precursor protein. kDa, kilo-Daltons.

Aβ*56 derived from Tg2576 mice impairs memory function when injected into the hippocampus

Although the initial appearance of Aβ*56 in Tg2576 mice at 6 months of age (Figure 1C) corresponds closely with the onset of impaired spatial reference memory,[34] it is possible that this coincidence is not due to a direct effect of Aβ*56 but instead results from a shared association with an independent factor. We addressed this possibility by directly assaying the effects of purified Aβ*56 injected into the hippocampus on memory function.

First, we isolated Aβ*56 from aqueous brain extracts from 17- to 22-month-old Tg2576 mice through immunoaffinity purification combined with SDS-PAGE/electro-elution techniques. Western blotting confirmed that the injectate contained Aβ*56 but no other Aβ entities (Figure 6A). We estimated the amount of Aβ*56 present to be 3.9 ng/μL by comparing its intensity with known quantities of Aβ monomers (Figure 6B). Assuming that each Aβ*56 oligomer bound only one 82E1 antibody, we estimated that the molar concentration of Aβ*56 in the injectate was 70 nM. A silver stain of the injectate showed no other bands (Figure 6C).

Next, we injected the left and right hippocampus of 4- to 7-month-old healthy FVB129S6 mice, each with 0.5 μL (1.95 ng) Aβ*56 or 0.5 μL phosphate-buffered saline (PBS) (Figure 6D). We tested memory function 23 h later using an object recognition test (ORT). The ORT, also called the novel object recognition test, was first described in 1988 by Ennaceur and Delacour.[35] We selected this test due to its simplicity, as it involves only one learning trial and one testing trial and can be completed in a single day.

We defined a discrimination index (DI) as the fraction of time a mouse explored the novel object during the testing trial relative to the total exploration time of both the familiar and novel objects. We found that the DIs of mice injected with Aβ*56 were significantly lower than those of mice injected with PBS ($U = 19$, $p = 0.0159$; two-tailed Mann-Whitney U test) (Figure 6E). We concluded that Aβ*56 potently impairs memory function at nanomolar injectate concentrations.

Aβ*56 entities produced in different APP transgenic lines are composed of different Aβ species

To investigate the presence of Aβ*56 in AD mouse models beyond Tg2576, we conducted experiments on aqueous brain extracts from 9-month-old 5xFAD and 10- to 11-month-old APP/TTA mice by IP with D8Q71 [anti-Aβ(x-40) antibody] or D3E10 [anti-Aβ(x-42) antibody], fractionation by SDS-PAGE, and western blotting with biotinylated 82E1 (anti-Aβ(1-x) antibody) (Figure 7A). In the case of 5xFAD mice, which express APP with the Swedish, Florida, and London mutations, along with two human presenilin-1 mutations,[36] we found that Aβ*56 was primarily composed of Aβ(x-42), not Aβ(x-40) (Figures 7B and 7C). For clarity, we have termed this particular variant Aβ(42)*56. In addition, our research revealed that Aβ(40)*56 and Aβ(42)*56 were both present in the APP/TTA mouse model expressing APP with the Swedish and Indiana mutations[37] (Figures 7D and 7E). The distinct expression patterns of these Aβ*56 variants in different AD mouse models are likely related to the varying levels and types of monomeric Aβ substrates produced in these models.

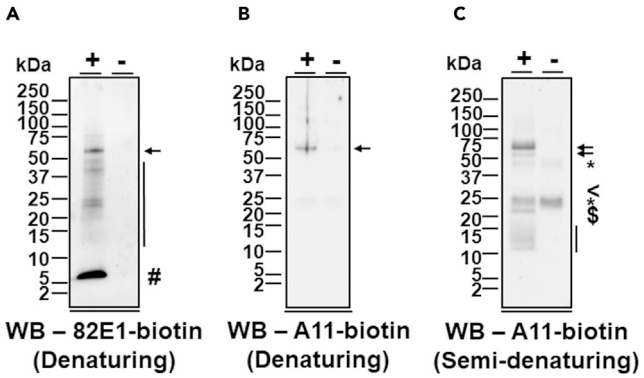

Figure 5. Immunopurified Aβ*56 is SDS-stable, contains canonical Aβ(1-40), and is recognized by A11, anti-oligomer antibodies

(A) A representative western blotting (WB) analysis showing under sodium dodecyl sulfate (SDS) denaturing conditions the detection of the ~56-kDa, D8Q7I-purified, 82E1-reactive entities (arrow), monomeric Aβ (#), and multiple entities of intermediate sizes (10–50 kDa, vertical line) in the brains of 15- to 22-month-old Tg2576 mice (+) but not age-matched littermates (–).

(B) A representative WB analysis showing that under SDS denaturing conditions, the ~56-kDa, D8Q7I-purified entities (arrow), but no other entities, bind to the biotinylated anti-oligomer antibody A11 (A11-biotin) in the brains of 15- to 21-month-old Tg2576 mice (+) but not age-matched littermates (–).

(C) A representative WB analysis showing that under SDS semi-denaturing conditions, the D8Q7I-purified, ~56-kDa (arrows), ~27-kDa (<), ~22-kDa ($), and ~10-15-kDa (vertical line) entities are reactive to biotinylated anti-oligomer antibody A11 (A11-biotin) in the brains of 15- to 22-month-old Tg2576 mice (+) but not age-matched littermates (–). kDa, kilo-Daltons. *non-specifically detected entities. See also Figures S38 and S39; Tables S1, S2, and S3.

DISCUSSION

In this paper, we show that Aβ*56 is a ~56-kDa, A11-reactive, SDS-stable, water-soluble, non-plaque-dependent, brain-derived oligomer that contains canonical Aβ(1-40) and/or Aβ(1-42) in different lines of APP transgenic mice. Within the detection limits of our assay, Aβ*56 in Tg2576 mice contains canonical Aβ(1-40), whereas in 5xFAD it contains Aβ(1-42). APP/TTA mice produce Aβ*56 that contains both Aβ(1-40) and Aβ(1-42). Aβ*56 purified from Tg2576 mice and injected into the brains of healthy, adult mice impairs memory function. Aβ*56 is the only consistently present, high molecular weight, SDS-stable, brain-derived oligomer that we were able to detect using the current experimental settings. We found that Aβ*56 can be sufficiently stable such that it does not undergo noticeable changes in conformation or size when boiled in reducing agents and exposed to SDS. To our knowledge, no other high-molecular-weight Aβ oligomers exhibiting this degree of stability have been described.

The term Aβ* pays homage to Charles Weissmann's moniker for a hypothetical form of the prion protein (PrP) that is "an infectious entity [which] could be a subspecies of PrP^{Sc} or a different modification of PrP altogether (which one might call PrP*)."[38] Conceptually an essential component of the prion, PrP* is by definition neurotoxic and could potentially be involved in the replication of prions.[39] More recent studies indicate, however, that prion neurotoxicity and infectivity can be dissociated.[40] In keeping with PrP*, Aβ*56 appears to be neurotoxic and associates closely with impaired memory,[1,17,18,20,21,23,25,27–29,41] but whether it is involved in the replication, aggregation, or propagation of Aβ is unclear. Aβ*56 is an A11-reactive oligomer but has not yet been shown to behave like synthetic, A11-reactive, "prefibrillar" or α-sheet-binding Aβ oligomers in solution, which evolve to become A11-negative, fibrillar oligomers and fibrils.[42,43] To explain the inverse relationships between insoluble Aβ and memory function that are observed only when mice are stratified by age, Westerman et al. postulated the existence of a soluble, intermediate Aβ aggregate in Tg2576 mice that both impairs memory and facilitates the production of insoluble Aβ species and amyloid plaques.[34] Clarifying the relationship between this hypothetical Aβ intermediate and Aβ*56 will require further investigation.

Although many groups have successfully studied Aβ*56 in mice,[1,17,20,23,25,27–29] aging dogs,[18] and humans diagnosed with AD,[21,41] detecting Aβ*56 can be challenging because it is rare (~2,880 ng per g wet forebrain mass of 17- to 22-month-old, neuritic-plaque-bearing Tg2576 mice; calculations in the "purification of Aβ*56" subsection of the method details under STAR Methods). We have found that high background and non-specific binding are the greatest impediments to accurate detection. In the current studies, we have modified the original protocol developed 20 years ago to reduce non-specific signals. Using this protocol, an independent laboratory detected Aβ*56 without difficulty (Figure S40). It is worth mentioning a few examples of the kinds of optimized experimental parameters that enhance the sensitivity and specificity of signals sufficiently to detect Aβ*56 reliably. We adjusted the buffers used to extract proteins, because we found that extracts containing detergents form irreversible, insoluble precipitates and may contain membrane-associated proteins. We found that tricine in gels accentuates the compactness of the Aβ*56 band; the corresponding bands in gels lacking tricine are more diffuse and less intense. The use of monoclonal antibodies that have been purified using protein A to capture proteins obscures Aβ*56 due to a non-specific band at ~50 kDa caused by protein A contaminants in the precipitated proteins.[44] The low concentrations of Aβ*56, which comprise less than 1% of total soluble Aβ in 20 months Tg2576 mice,[2] necessitate taking advantage of the greater sensitivity of biotin-avidin coupled to chemiluminescence compared with colorimetric methods. It is important to beware that some batches of A11 do not detect Aβ*56 (Figure S39).

We surmise, based on comparing banding patterns in our current western blots with those in the literature, that the Aβ*56 entity we describe here overlaps with but may not correspond exactly to the ~56-kDa entities that have been identified using other protocols. Technical refinements permit more accurate characterizations of Aβ assemblies. For example, the constituents of highly neurotoxic entities in 7PA2

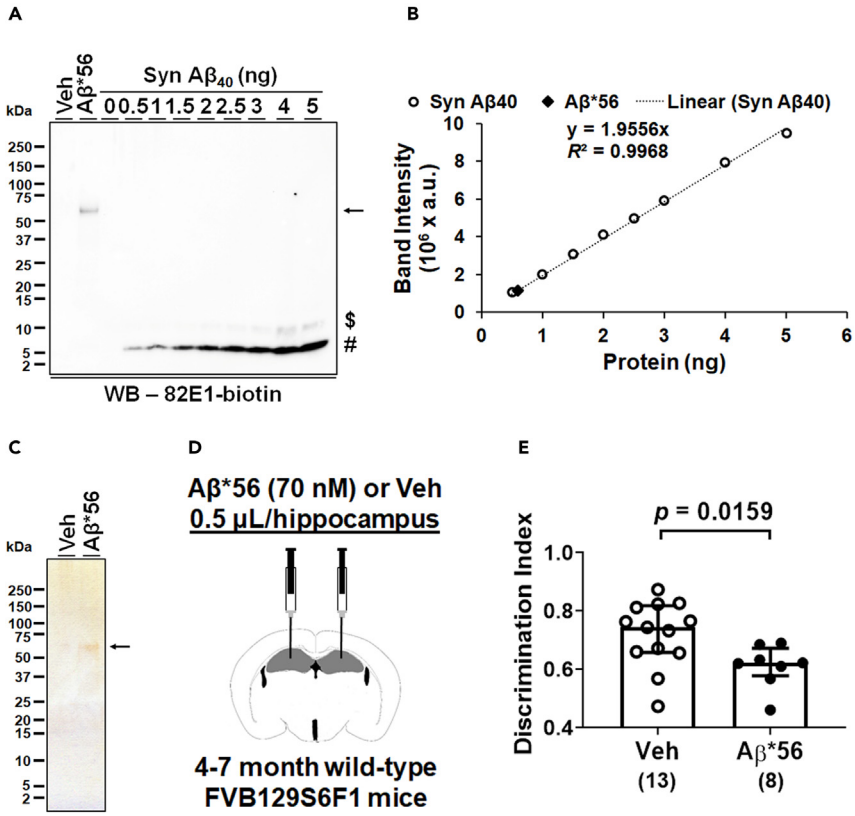

Figure 6. Aβ*56 isolated from Tg2576 mice impairs memory function

(A) A representative western blotting (WB) analysis showing the detection of Aβ*56 isolated from brains of 17- to 22-month-old Tg2576 mice following immunoaffinity purification coupled to SDS-PAGE/electro-elution. The quantity and purity of isolated Aβ*56 (arrow, 2 µL loaded) used for surgical injection and mouse memory tests (D and E) were assessed by WB with various amounts of synthetic monomeric Aβ(1-40) (Syn $Aβ_{40}$) serving as quantification standards. Aβ*56, but no other Aβ species, is detected by biotinylated 82E1 (82E1-biotin). #, monomeric Aβ(1-40); and $, dimeric Aβ(1-40).

(B) Densitometry-based quantification of Aβ*56. The linear relationship between the amounts of 82E1-reactive proteins and band intensities in (A) was established using synthetic Aβ(1-40) standards. By fitting the band intensity of Aβ*56 to the standard curve, the concentration of Aβ*56 was determined to be 3.9 ng/µL (i.e., 70 nM, assuming that the stoichiometry of 82E1 binding to monomeric Aβ(1-40) is equal to that of 82E1 binding to Aβ*56).

(C) A representative silver stain analysis assessing the purity of isolated Aβ*56 (arrow, 5 µL loaded) used for the study of mouse memory (D and E).

(D) A schematic illustration of bilateral intra-hippocampal injections of Aβ*56.

(E) Healthy 4- to 7-month-old wild-type mice injected with Aβ*56 exhibit lower (U = 19, p = 0.0159; two-tailed Mann-Whitney U test) discrimination indices compared with those injected with vehicle (phosphate-buffered saline) in an object recognition test. The scatter plot with bar graph represents data of individual mice plus group median ± interquartile range. The numbers of mice used for the vehicle and Aβ*56 groups are shown in parentheses. Veh, vehicle; kDa, kilo-Dalton.

culture medium originally believed to be dimers and trimers[45] were found upon later investigation also to contain N-terminally extended, non-canonical Aβ.[46] Although our current protocol reliably and reproducibly detects Aβ*56, we anticipate that continued, methodological advancements will enable future investigations of Aβ*56 to be conducted more efficiently.

Not all lines of mice produce Aβ*56. The levels and species of Aβ generated in a particular line of mice affect the expression of Aβ*56. For example, Tg2576 mice expressing APP-Swe express Aβ*56 but rTg9191 mice expressing APP-Swe with the V717I London mutation that promotes fibril formation do not.[2,30] The balance between aggregation processes that do (on-pathway) and do not (off-pathway) culminate in fibrils may influence the production of Aβ*56, as the two pathways may compete for monomers in a common pool.

The structure, spatial distribution, and temporal expression of Aβ oligomers are important determinants of their effects on the brain.[2,47] Two distinctive spatial and temporal features of Aβ*56 are that it forms before dense-core plaques and is present within, but not confined to, dense-core plaques.[1,2] This is significant, because in mice the oligomers that are confined to dense-core plaques do not impair neurological function unless they are burst open and dispersed in the brain.[2] Although the precise structure of Aβ*56 is unknown, some general features may be deduced from binding studies using the polyclonal, conformational antibodies, OC and A11.[4,7] OC antibodies, which recognize in-register, parallel β-sheets, and to a lesser extent antiparallel β-sheets, do not bind Aβ*56[2]. A11 antibodies, which recognize a variety of conformational epitopes, bind Aβ*56 in mice[1,20] (and this paper), dogs,[18] and humans,[21,48] but the specific epitope(s) recognized is unknown. Because A11 antibodies

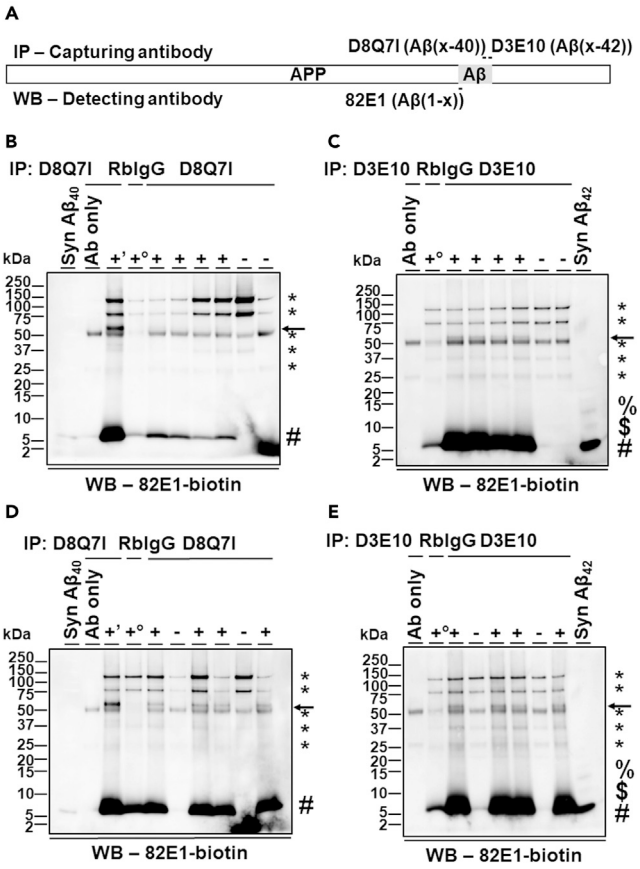

Figure 7. Aβ*56 is present in two other mouse models of AD

(A) A schematic illustration of epitopes of capturing and detecting antibodies used in immunoprecipitation (IP)/western blotting (WB) for (B–E). Capturing antibody: rabbit monoclonal D8Q7I that is directed against the C-terminus of Aβ(x-40) or rabbit monoclonal D3E10 that is directed against the C-terminus of Aβ(x-42), detecting antibody: biotinylated mouse monoclonal 82E1 that is directed against the N-terminus of Aβ(1-x). APP, amyloid precursor protein; Aβ, amyloid-β.

(B) Representative IP/WB analyses showing that D8Q7I-precipitated entities electrophoresed at ~56 kDa (arrow) are detected by biotinylated 82E1 (82E1-biotin) in 17-month-old Tg2576 (+') mice (serving as a positive control for IP/WB) but not in 9-month-old 5xFAD (+) mice, in age-matched non-transgenic littermates (–) of 5xFAD mice, or when no brain extracts were used (Ab only). No ~56-kDa entities are detected when generic rabbit immunoglobulin G (RbIgG) was used to precipitate brain extracts (+°, combined brain extracts of the four 5xFAD mice, each contributing 25% of the total proteins). Ab, capturing antibody D8Q7I. Syn $A\beta_{40}$, synthetic Aβ(1-40) (1 ng), serving as a positive control for WB. #, monomeric Aβ(x-40).

(C) Representative IP/WB analyses showing that D3E10-precipitated entities electrophoresed at ~56 kDa (arrow) are detected by 82E1-biotin in 9-month-old 5xFAD (+) mice but not in age-matched non-transgenic littermates (–) of 5xFAD mice or when no brain extracts were used (Ab only). No ~56-kDa entities are detected when RbIgG was used to precipitate brain extracts (+°, combined brain extracts of the four 5xFAD mice, each contributing 25% of the total proteins). Ab, capturing antibody D3E10. Syn $A\beta_{42}$, synthetic Aβ(1-42) (5 ng), serving as a positive control for WB. #, monomeric Aβ(x-42); $, dimeric Syn $A\beta_{42}$; @, trimeric Syn $A\beta_{42}$.

(D) Representative IP/WB analyses showing that D8Q7I-precipitated entities electrophoresed at ~56 kDa (arrow) are detected by 82E1-biotin in 17-month-oldTg2576 (+', serving as a positive control for IP/WB) and 10- to 11-month-old APP/TTA (+) mice but not in age-matched non-transgenic littermates (–) of APP/TTA mice or when no brain extracts were used (Ab only). No ~56-kDa entities are detected when RbIgG was used to precipitate brain extracts (+°, combined brain extracts of the four APP/TTA mice, each contributing 25% of the total proteins). Ab, capturing antibody D8Q7I. Syn $A\beta_{40}$, synthetic Aβ(1-40) (1 ng), serving as a positive control for WB. #, monomeric Aβ(x-40).

(E) Representative IP/WB analyses showing that D3E10-precipitated entities electrophoresed at ~56 kDa (arrow) are detected by 82E1-biotin in 10- to 11-month-old APP/TTA (+) mice but not in age-matched non-transgenic littermates (–) of APP/TTA mice or when no brain extracts were used (Ab only). No ~56-kDa entities are detected when RbIgG was used to precipitate brain extracts (+°, combined brain extracts of the four APP/TTA mice, each contributing 25% of the total proteins). Ab, capturing antibody D3E10. Syn $A\beta_{42}$, synthetic Aβ(1-42) (5 ng), serving as a positive control for WB. #, monomeric Aβ(x-42); $, dimeric Syn $A\beta_{42}$; @, trimeric Syn $A\beta_{42}$. For (B–E), *, non-specifically detected entities and kDa, kilo-Daltons.

are polyclonal, more than one A11-reactive variant may be present, complicating the ability to decipher the structural properties of Aβ*56. Currently, there are no monoclonal, conformational antibodies that selectively bind Aβ*56.

In summary, in this paper, we confirmed and extended the characterization of a ~56-kDa, A11-binding, SDS-stable, water-soluble, non-plaque-dependent, brain-derived oligomer, also known as Aβ*56, and found that it contains canonical Aβ(1-40) and/or Aβ(1-42). We showed

that Aβ*56 purified from Tg2576 mice impairs memory when injected into the brains of healthy mice. We provided detailed information about the techniques, tools, and specimens that enable Aβ*56 to be detected reliably and reproducibly.

Limitations of the study

Although the current studies are limited to mice, it is likely that Aβ*56 is present in humans. One group previously reported detecting higher levels of A11-reactive, ~56-kDa entities in nasal fluid from humans with AD.[21,41] We previously described an isolated cluster of ~56-kDa, 82E1-reactive bands on a western blot of immunoprecipitated Aβ(x-40)/Aβ(x-42) proteins from human cerebrospinal fluid (CSF).[49] When the immunoprecipitated CSF proteins were probed using 6E10 antibodies, however, non-oligomeric, APP fragments were also detected,[49] illustrating the importance of employing antibodies that specifically detect canonical Aβ. An earlier study using 6E10 antibodies reported paradoxically lower levels of Aβ*56 in brain tissue from AD patients,[48] which may have resulted from the inadvertent contribution of 6E10-binding APP fragments to the measurements. Using our current protocols to examine Aβ*56 levels in AD, our preliminary results suggest that Aβ*56 is elevated in AD (I. Lapcinski and P. Liu, unpublished findings).

Although we did not observe any SDS-stable Aβ oligomers larger than 100 kDa, we cannot exclude their existence because our experimental protocol is optimized to detect oligomers smaller than 100 kDa. Optimized experimental parameters are needed to investigate the existence of larger, SDS-stable oligomers.

STAR★METHODS

Detailed methods are provided in the online version of this paper and include the following:

- KEY RESOURCES TABLE
- RESOURCE AVAILABILITY
  - Lead contact
  - Materials availability
  - Data and code availability
- EXPERIMENTAL MODEL AND STUDY PARTICIPANT DETAILS
  - Animals
  - Tg2576
  - 5xFAD
  - APP/TTA
  - rTg9191
  - Wild-type mice
- METHOD DETAILS
  - Antibodies
  - Brain protein extraction
  - Size-exclusion chromatography (SEC)
  - Immunoprecipitation (IP)
  - Western blotting (WB)
  - Denaturant treatment
  - Antibody immobilization on Dynabeads
  - Immunoaffinity purification
  - Purification of Aβ*56
  - Silver stain
  - Object recognition test (ORT)
  - Aβ*56 injection into brains of wild-type mice
- QUANTIFICATION AND STATISTICAL ANALYSIS

SUPPLEMENTAL INFORMATION

Supplemental information can be found online at https://doi.org/10.1016/j.isci.2024.109239.

ACKNOWLEDGMENTS

Biochemistry studies were supported using funds from the N. Bud Grossman Center for Memory Research and Care and a Metropolitan Life Prize for Alzheimer's Research awarded to K.H.A. The authors thank Dr. Swathy Babu and Dr. Shauna Yuan, University of Minnesota, Twin Cities, Minnesota, for contributing Fig. S40; Dr. Joanna Jankowsky, Baylor College of Medicine, Houston, Texas, for providing brain specimens of 5xFAD and APP/TTA mice; Dr. George Carlson, McLaughlin Research Institute, Great Falls, Montana, for providing brain specimens of rTg9191 mice; and Dr. Dominic Walsh, Brigham and Women's Hospital, Boston, Massachusetts, for providing the HJ2 and HJ7.4 antibodies.

AUTHOR CONTRIBUTIONS

P.L. conceived the study, designed and performed biochemistry experiments, analyzed data, and wrote the manuscript. I.P.L. and S.L.S. helped design and perform biochemistry experiments and analyzed data. C.J.W.H. and T.J.L. performed intra-hippocampal injections. E.L.S. and L.J.K. conducted the ORT. K.H.A. conceived the study, analyzed data, and wrote the manuscript.

DECLARATION OF INTERESTS

The authors declare no competing interests.

Received: March 20, 2023
Revised: December 12, 2023
Accepted: February 11, 2024
Published: February 15, 2024

REFERENCES

1. Lesné, S., Koh, M.T., Kotilinek, L., Kayed, R., Glabe, C.G., Yang, A., Gallagher, M., and Ashe, K.H. (2006). A specific amyloid-beta protein assembly in the brain impairs memory. Nature *440*, 352–357. https://doi.org/10.1038/nature04533.
2. Liu, P., Reed, M.N., Kotilinek, L.A., Grant, M.K.O., Forster, C.L., Qiang, W., Shapiro, S.L., Reichl, J.H., Chiang, A.C.A., Jankowsky, J.L., et al. (2015). Quaternary Structure Defines a Large Class of Amyloid-beta Oligomers Neutralized by Sequestration. Cell Rep. *11*, 1760–1771. https://doi.org/10.1016/j.celrep.2015.05.021.
3. Roher, A.E., Chaney, M.O., Kuo, Y.M., Webster, S.D., Stine, W.B., Haverkamp, L.J., Woods, A.S., Cotter, R.J., Tuohy, J.M., Krafft, G.A., et al. (1996). Morphology and toxicity of Abeta-(1-42) dimer derived from neuritic and vascular amyloid deposits of Alzheimer's disease. J. Biol. Chem. *271*, 20631–20635. https://doi.org/10.1074/jbc.271.34.20631.
4. Kayed, R., Head, E., Thompson, J.L., McIntire, T.M., Milton, S.C., Cotman, C.W., and Glabe, C.G. (2003). Common structure of soluble amyloid oligomers implies common mechanism of pathogenesis. Science *300*, 486–489. https://doi.org/10.1126/science.1079469.
5. Hoshi, M., Sato, M., Matsumoto, S., Noguchi, A., Yasutake, K., Yoshida, N., and Sato, K. (2003). Spherical aggregates of beta-amyloid (amylospheroid) show high neurotoxicity and activate tau protein kinase I/glycogen synthase kinase-3beta. Proc. Natl. Acad. Sci. USA *100*, 6370–6375. https://doi.org/10.1073/pnas.1237107100.
6. Barghorn, S., Nimmrich, V., Striebinger, A., Krantz, C., Keller, P., Janson, B., Bahr, M., Schmidt, M., Bitner, R.S., Harlan, J., et al. (2005). Globular amyloid beta-peptide oligomer - a homogenous and stable neuropathological protein in Alzheimer's disease. J. Neurochem. *95*, 834–847. https://doi.org/10.1111/j.1471-4159.2005.03407.x.
7. Kayed, R., Head, E., Sarsoza, F., Saing, T., Cotman, C.W., Necula, M., Margol, L., Wu, J., Breydo, L., Thompson, J.L., et al. (2007). Fibril specific, conformation dependent antibodies recognize a generic epitope common to amyloid fibrils and fibrillar oligomers that is absent in prefibrillar oligomers. Mol. Neurodegener. *2*, 18. https://doi.org/10.1186/1750-1326-2-18.
8. Englund, H., Sehlin, D., Johansson, A.S., Nilsson, L.N.G., Gellerfors, P., Paulie, S., Lannfelt, L., and Pettersson, F.E. (2007). Sensitive ELISA detection of amyloid-beta protofibrils in biological samples. J. Neurochem. *103*, 334–345. https://doi.org/10.1111/j.1471-4159.2007.04759.x.
9. Tomiyama, T., Matsuyama, S., Iso, H., Umeda, T., Takuma, H., Ohnishi, K., Ishibashi, K., Teraoka, R., Sakama, N., Yamashita, T., et al. (2010). A mouse model of amyloid beta oligomers: their contribution to synaptic alteration, abnormal tau phosphorylation, glial activation, and neuronal loss in vivo. J. Neurosci. *30*, 4845–4856. https://doi.org/10.1523/JNEUROSCI.5825-09.2010.
10. Lasagna-Reeves, C.A., Glabe, C.G., and Kayed, R. (2011). Amyloid-beta annular protofibrils evade fibrillar fate in Alzheimer disease brain. J. Biol. Chem. *286*, 22122–22130. https://doi.org/10.1074/jbc.M111.236257.
11. Serra-Batiste, M., Ninot-Pedrosa, M., Bayoumi, M., Gairí, M., Maglia, G., and Carulla, N. (2016). Abeta42 assembles into specific beta-barrel pore-forming oligomers in membrane-mimicking environments. Proc. Natl. Acad. Sci. USA *113*, 10866–10871. https://doi.org/10.1073/pnas.1605104113.
12. Adolfsson, O., Pihlgren, M., Toni, N., Varisco, Y., Buccarello, A.L., Antoniello, K., Lohmann, S., Piorkowska, K., Gafner, V., Atwal, J.K., et al. (2012). An effector-reduced anti-beta-amyloid (Abeta) antibody with unique abeta binding properties promotes neuroprotection and glial engulfment of Abeta. J. Neurosci. *32*, 9677–9689. https://doi.org/10.1523/JNEUROSCI.4742-11.2012.
13. Sevigny, J., Chiao, P., Bussière, T., Weinreb, P.H., Williams, L., Maier, M., Dunstan, R., Salloway, S., Chen, T., Ling, Y., et al. (2016). The antibody aducanumab reduces Abeta plaques in Alzheimer's disease. Nature *537*, 50–56. https://doi.org/10.1038/nature19323.
14. Krafft, G.A., Jerecic, J., Siemers, E., and Cline, E.N. (2022). ACU193: An Immunotherapeutic Poised to Test the Amyloid beta Oligomer Hypothesis of Alzheimer's Disease. Front. Neurosci. *16*, 848215. https://doi.org/10.3389/fnins.2022.848215.
15. Shea, D., Colasurdo, E., Smith, A., Paschall, C., Jayadev, S., Keene, C.D., Galasko, D., Ko, A., Li, G., Peskind, E., and Daggett, V. (2022). SOBA: Development and testing of a soluble oligomer binding assay for detection of amyloidogenic toxic oligomers. Proc. Natl. Acad. Sci. USA *119*, e2213157119. https://doi.org/10.1073/pnas.2213157119.
16. Gil, B., Rose, J., Demurtas, D., Mancini, G.-F., Sordet-Dessimoz, F., Sorrentino, V., Rudinskiy, N., Frosch, M.P., Human, B.T., Moniatte, M., et al. (2023). Elucidation of Amyloid-Beta's Gambit in Oligomerization: Truncated Aβ fragments of residues Aβ1-23, Aβ1-24 and Aβ1-25 rapidly seed to form SDS-stable, LMW Aβ oligomers that impair synaptic plasticity. Preprint at bioRxiv. https://doi.org/10.1101/2022.12.04.519021.
17. Billings, L.M., Green, K.N., McGaugh, J.L., and LaFerla, F.M. (2007). Learning decreases A beta*56 and tau pathology and ameliorates behavioral decline in 3xTg-AD mice. J. Neurosci. *27*, 751–761. https://doi.org/10.1523/JNEUROSCI.4800-06.2007.
18. Pop, V., Head, E., Berchtold, N.C., Glabe, C.G., Studzinski, C.M., Weidner, A.M., Murphy, M.P., and Cotman, C.W. (2012). Abeta aggregation profiles and shifts in APP processing favor amyloidogenesis in canines. Neurobiol. Aging *33*, 108–120. https://doi.org/10.1016/j.neurobiolaging.2010.02.008.
19. Hsiao, K., Chapman, P., Nilsen, S., Eckman, C., Harigaya, Y., Younkin, S., Yang, F., and Cole, G. (1996). Correlative memory deficits, Abeta elevation, and amyloid plaques in transgenic mice. Science *274*, 99–102.
20. Yoo, S.J., Lee, J.H., Kim, S.Y., Son, G., Kim, J.Y., Cho, B., Yu, S.W., Chang, K.A., Suh, Y.H., and Moon, C. (2017). Differential spatial expression of peripheral olfactory neuron-derived BACE1 induces olfactory impairment by region-specific accumulation of beta-amyloid oligomer. Cell Death Dis. *8*, e2977. https://doi.org/10.1038/cddis.2017.349.
21. Yoo, S.J., Son, G., Bae, J., Kim, S.Y., Yoo, Y.K., Park, D., Baek, S.Y., Chang, K.A., Suh, Y.H., Lee, Y.B., et al. (2020). Longitudinal profiling of oligomeric Abeta in human nasal discharge reflecting cognitive decline in probable Alzheimer's disease. Sci. Rep. *10*, 11234. https://doi.org/10.1038/s41598-020-68148-2.
22. Mucke, L., Masliah, E., Yu, G.Q., Mallory, M., Rockenstein, E.M., Tatsuno, G., Hu, K., Kholodenko, D., Johnson-Wood, K., and McConlogue, L. (2000). High-level neuronal expression of abeta 1-42 in wild-type human amyloid protein precursor transgenic mice: synaptotoxicity without plaque formation. J. Neurosci. *20*, 4050–4058. https://doi.org/10.1523/JNEUROSCI.20-11-04050.2000.
23. Cheng, I.H., Scearce-Levie, K., Legleiter, J., Palop, J.J., Gerstein, H., Bien-Ly, N., Puoliväli, J., Lesné, S., Ashe, K.H., Muchowski, P.J., and Mucke, L. (2007). Accelerating amyloid-beta fibrillization reduces oligomer levels and functional deficits in Alzheimer disease mouse

models. J. Biol. Chem. *282*, 23818–23828. https://doi.org/10.1074/jbc.M701078200.
24. Cheng, I.H., Palop, J.J., Esposito, L.A., Bien-Ly, N., Yan, F., and Mucke, L. (2004). Aggressive amyloidosis in mice expressing human amyloid peptides with the Arctic mutation. Nat. Med. *10*, 1190–1192. https://doi.org/10.1038/nm1123.
25. Meilandt, W.J., Cisse, M., Ho, K., Wu, T., Esposito, L.A., Scearce-Levie, K., Cheng, I.H., Yu, G.Q., and Mucke, L. (2009). Neprilysin overexpression inhibits plaque formation but fails to reduce pathogenic Abeta oligomers and associated cognitive deficits in human amyloid precursor protein transgenic mice. J. Neurosci. *29*, 1977–1986. https://doi.org/10.1523/JNEUROSCI.2984-08.2009.
26. Wang, J., Ho, L., Zhao, W., Ono, K., Rosensweig, C., Chen, L., Humala, N., Teplow, D.B., and Pasinetti, G.M. (2008). Grape-derived polyphenolics prevent Abeta oligomerization and attenuate cognitive deterioration in a mouse model of Alzheimer's disease. J. Neurosci. *28*, 6388–6392. https://doi.org/10.1523/JNEUROSCI.0364-08.2008.
27. Liu, P., Kemper, L.J., Wang, J., Zahs, K.R., Ashe, K.H., and Pasinetti, G.M. (2011). Grape seed polyphenolic extract specifically decreases abeta*56 in the brains of Tg2576 mice. J. Alzheimers Dis. *26*, 657–666. https://doi.org/10.3233/JAD-2011-110383.
28. Castillo-Carranza, D.L., Guerrero-Muñoz, M.J., Sengupta, U., Hernandez, C., Barrett, A.D.T., Dineley, K., and Kayed, R. (2015). Tau immunotherapy modulates both pathological tau and upstream amyloid pathology in an Alzheimer's disease mouse model. J. Neurosci. *35*, 4857–4868. https://doi.org/10.1523/JNEUROSCI.4989-14.2015.
29. Fowler, S.W., Chiang, A.C.A., Savjani, R.R., Larson, M.E., Sherman, M.A., Schuler, D.R., Cirrito, J.R., Lesné, S.E., and Jankowsky, J.L. (2014). Genetic modulation of soluble Abeta rescues cognitive and synaptic impairment in a mouse model of Alzheimer's disease. J. Neurosci. *34*, 7871–7885. https://doi.org/10.1523/JNEUROSCI.0572-14.2014.
30. Liu, P., Paulson, J.B., Forster, C.L., Shapiro, S.L., Ashe, K.H., and Zahs, K.R. (2015). Characterization of a Novel Mouse Model of Alzheimer's Disease–Amyloid Pathology and Unique beta-Amyloid Oligomer Profile. PLoS One *10*, e0126317. https://doi.org/10.1371/journal.pone.0126317.
31. Callahan, M.J., Lipinski, W.J., Bian, F., Durham, R.A., Pack, A., and Walker, L.C. (2001). Augmented senile plaque load in aged female beta-amyloid precursor protein-transgenic mice. Am. J. Pathol. *158*, 1173–1177. https://doi.org/10.1016/s0002-9440(10)64064-3.
32. Snyder, S.W., Ladror, U.S., Wade, W.S., Wang, G.T., Barrett, L.W., Matayoshi, E.D., Huffaker, H.J., Krafft, G.A., and Holzman, T.F. (1994). Amyloid-beta aggregation: selective inhibition of aggregation in mixtures of amyloid with different chain lengths. Biophys. J. *67*, 1216–1228. https://doi.org/10.1016/S0006-3495(94)80591-0.
33. Esparza, T.J., Wildburger, N.C., Jiang, H., Gangolli, M., Cairns, N.J., Bateman, R.J., and Brody, D.L. (2016). Soluble Amyloid-beta Aggregates from Human Alzheimer's Disease Brains. Sci. Rep. *6*, 38187. https://doi.org/10.1038/srep38187.
34. Westerman, M.A., Cooper-Blacketer, D., Mariash, A., Kotilinek, L., Kawarabayashi, T., Younkin, L.H., Carlson, G.A., Younkin, S.G., and Ashe, K.H. (2002). The relationship between Abeta and memory in the Tg2576 mouse model of Alzheimer's disease. J. Neurosci. *22*, 1858–1867.
35. Ennaceur, A., and Delacour, J. (1988). A new one-trial test for neurobiological studies of memory in rats. 1: Behavioral data. Behav. Brain Res. *31*, 47–59. https://doi.org/10.1016/0166-4328(88)90157-x.
36. Oakley, H., Cole, S.L., Logan, S., Maus, E., Shao, P., Craft, J., Guillozet-Bongaarts, A., Ohno, M., Disterhoft, J., Van Eldik, L., et al. (2006). Intraneuronal beta-amyloid aggregates, neurodegeneration, and neuron loss in transgenic mice with five familial Alzheimer's disease mutations: potential factors in amyloid plaque formation. J. Neurosci. *26*, 10129–10140. https://doi.org/10.1523/JNEUROSCI.1202-06.2006.
37. Jankowsky, J.L., Slunt, H.H., Gonzales, V., Savonenko, A.V., Wen, J.C., Jenkins, N.A., Copeland, N.G., Younkin, L.H., Lester, H.A., Younkin, S.G., and Borchelt, D.R. (2005). Persistent amyloidosis following suppression of Abeta production in a transgenic model of Alzheimer disease. PLoS Med. *2*, e355. https://doi.org/10.1371/journal.pmed.0020355.
38. Weissmann, C. (1991). Spongiform encephalopathies. The prion's progress. Nature *349*, 569–571. https://doi.org/10.1038/349569a0.
39. Weissmann, C. (2004). The state of the prion. Nat. Rev. Microbiol. *2*, 861–871. https://doi.org/10.1038/nrmicro1025.
40. Benilova, I., Reilly, M., Terry, C., Wenborn, A., Schmidt, C., Marinho, A.T., Risse, E., Al-Doujaily, H., Wiggins De Oliveira, M., Sandberg, M.K., et al. (2020). Highly infectious prions are not directly neurotoxic. Proc. Natl. Acad. Sci. USA *117*, 23815–23822. https://doi.org/10.1073/pnas.2007406117.
41. Sokolow, S., Henkins, K.M., Bilousova, T., Miller, C.A., Vinters, H.V., Poon, W., Cole, G.M., and Gylys, K.H. (2012). AD synapses contain abundant Abeta monomer and multiple soluble oligomers, including a 56-kDa assembly. Neurobiol. Aging *33*, 1545–1555. https://doi.org/10.1016/j.neurobiolaging.2011.05.011.
42. Shea, D., and Daggett, V. (2022). Amyloid-beta oligomers: multiple moving targets. Biophysica *2*, 91–110.
43. Glabe, C.G. (2008). Structural classification of toxic amyloid oligomers. J. Biol. Chem. *283*, 29639–29643. https://doi.org/10.1074/jbc.R800016200.
44. Grant, M.K.O., Shapiro, S.L., Ashe, K.H., Liu, P., and Zahs, K.R. (2019). A Cautionary Tale: Endogenous Biotinylated Proteins and Exogenously-Introduced Protein A Cause Antibody-Independent Artefacts in Western Blot Studies of Brain-Derived Proteins. Biol. Proced. Online *21*, 6. https://doi.org/10.1186/s12575-019-0095-z.
45. Walsh, D.M., Klyubin, I., Fadeeva, J.V., Cullen, W.K., Anwyl, R., Wolfe, M.S., Rowan, M.J., and Selkoe, D.J. (2002). Naturally secreted oligomers of amyloid beta protein potently inhibit hippocampal long-term potentiation in vivo. Nature *416*, 535–539. https://doi.org/10.1038/416535a.
46. Welzel, A.T., Maggio, J.E., Shankar, G.M., Walker, D.E., Ostaszewski, B.L., Li, S., Klyubin, I., Rowan, M.J., Seubert, P., Walsh, D.M., and Selkoe, D.J. (2014). Secreted amyloid beta-proteins in a cell culture model include N-terminally extended peptides that impair synaptic plasticity. Biochemistry *53*, 3908–3921. https://doi.org/10.1021/bi5003053.
47. Ashe, K.H. (2020). The biogenesis and biology of amyloid beta oligomers in the brain. Alzheimers Dement. *16*, 1561–1567. https://doi.org/10.1002/alz.12084.
48. Lesné, S.E., Sherman, M.A., Grant, M., Kuskowski, M., Schneider, J.A., Bennett, D.A., and Ashe, K.H. (2013). Brain amyloid-beta oligomers in ageing and Alzheimer's disease. Brain *136*, 1383–1398. https://doi.org/10.1093/brain/awt062.
49. Grant, M.K.O., Handoko, M., Rozga, M., Brinkmalm, G., Portelius, E., Blennow, K., Ashe, K.H., Zahs, K.R., and Liu, P. (2019). Human cerebrospinal fluid 6E10-immunoreactive protein species contain amyloid precursor protein fragments. PLoS One *14*, e0212815. https://doi.org/10.1371/journal.pone.0212815.
50. Kotilinek, L.A., Westerman, M.A., Wang, Q., Panizzon, K., Lim, G.P., Simonyi, A., Lesne, S., Falinska, A., Younkin, L.H., Younkin, S.G., et al. (2008). Cyclooxygenase-2 inhibition improves amyloid-beta-mediated suppression of memory and synaptic plasticity. Brain *131*, 651–664. https://doi.org/10.1093/brain/awn008.
51. Shankar, G.M., Li, S., Mehta, T.H., Garcia-Munoz, A., Shepardson, N.E., Smith, I., Brett, F.M., Farrell, M.A., Rowan, M.J., Lemere, C.A., et al. (2008). Amyloid-beta protein dimers isolated directly from Alzheimer's brains impair synaptic plasticity and memory. Nat. Med. *14*, 837–842. https://doi.org/10.1038/nm1782.
52. Liu, P., Reichl, J.H., Rao, E.R., McNellis, B.M., Huang, E.S., Hemmy, L.S., Forster, C.L., Kuskowski, M.A., Borchelt, D.R., Vassar, R., et al. (2017). Quantitative Comparison of Dense-Core Amyloid Plaque Accumulation in Amyloid-beta Protein Precursor Transgenic Mice. J. Alzheimers Dis. *56*, 743–761. https://doi.org/10.3233/JAD-161027.
53. Liu, P., Smith, B.R., Montonye, M.L., Kemper, L.J., Leinonen-Wright, K., Nelson, K.M., Higgins, L., Guerrero, C.R., Markowski, T.W., Zhao, X., et al. (2020). A soluble truncated tau species related to cognitive dysfunction is elevated in the brain of cognitively impaired human individuals. Sci. Rep. *10*, 3869. https://doi.org/10.1038/s41598-020-60777-x.
54. Rupprecht, K.R., Lang, E.Z., Gregory, S.D., Bergsma, J.M., Rae, T.D., and Fishpaugh, J.R. (2015). A precise spectrophotometric method for measuring sodium dodecyl sulfate concentration. Anal. Biochem. *486*, 78–80. https://doi.org/10.1016/j.ab.2015.06.013.

STAR★METHODS

KEY RESOURCES TABLE

REAGENT or RESOURCE	SOURCE	IDENTIFIER
Antibodies		
Rabbit monoclonal anti-Aβ(x-40)	Cell Signaling Technology	Cat#12990S; Clone#D8Q7I; RRID: AB_2798082
Rabbit monoclonal biotinylated anti-Aβ(x-40)	This paper	N/A
Rabbit monoclonal anti-Aβ(x-42)	Cell Signaling Technology	Cat#12843S; Clone# D3E10; RRID: AB_2798041
Mouse monoclonal biotinylated anti-Aβ(3–8)	BioLegend	Cat#803009; Clone# 6E10; RRID: AB_2564656
Mouse monoclonal anti-Aβ(1-x)	IBL America	Cat#10323; Clone# 82E1; RRID: AB_10707424
Mouse monoclonal biotinylated anti-Aβ(1-x)	IBL America	Cat#10326; Clone# 82E1; RRID: AB_1540459
Mouse monoclonal anti-Aβ(x-40)	A kind gift from Dr. Dominic Walsh	Cat# MABN2422; Clone# mHJ2
Mouse monoclonal anti-Aβ(x-42)	A kind gift from Dr. Dominic Walsh	Cat# MABN2421; Clone# mHJ7.4
Rabbit polyclonal anti-amyloid oligomers	Rockland	Cat#200-401-E88; Clone#A11; RRID: AB_2612166
Rabbit polyclonal anti-amyloid oligomers	StressMarq Biosciences	Cat#SPC-506D; Clone#A11; RRID: AB_10962958
Rabbit polyclonal biotinylated anti-amyloid oligomers	StressMarq Biosciences	Cat#SPC-506D-BI; Clone#A11; RRID: AB_10962958
Rabbit polyclonal anti-amyloid oligomers	Invitrogen	Cat#AHB0052; Clone#A11; RRID: AB_2536236
Rabbit polyclonal anti-amyloid oligomers	MilliporeSigma	Cat#AB9234; Clone#A11; RRID: AB_570955
Biotin-SP (long spacer) AffiniPure donkey-anti-rabbit IgG (H+L)	Jackson ImmunoResearch Laboratories	711-065-152; RRID: AB_2340593
Biological samples		
Frozen forebrain tissue of Tg2576 mice (B6;SJL)	Dr. Karen Ashe laboratory	N/A
Frozen forebrain tissue of Tg2576 mice (129S6)	Dr. Karen Ashe laboratory	N/A
Frozen forebrain tissue of Tg2576 mice (129S6;FVB F1)	Dr. Karen Ashe laboratory	N/A
Frozen forebrain tissue of rTg9191 mice (FVB;129S6 F1)	A kind gift from Dr. George Carlson	N/A
Frozen forebrain tissue of 5xFAD mice (B6)	A kind gift from Dr. Joanna Jankowsky	N/A
Frozen forebrain tissue of APP/TTA mice (B6)	A kind gift from Dr. Joanna Jankowsky	N/A
Chemicals, peptides, and recombinant proteins		
Synthetic Aβ(1–40)	MilliporeSigma	Cat#A1075
Synthetic Aβ(1–42)	MilliporeSigma	Cat#A9810
Synthetic Aβ(pE3-42)	AnaSpec	Cat#AS-29907
Experimental models: Organisms/strains		
Mouse: Tg2576, B6;SJL-Tg(APPSWE) 2576Kha/Tac: B6;SJL	Hsiao et al.[19]	RRID:IMSR_TAC:1349
Mouse: Tg2576, 129S6.Cg-Tg(APPSWE) 2576Kha/Tac: 129S6	Westerman et al.[34]	RRID:MGI:4838309
Mouse: Tg2576, 129S6;FVB F1-Tg(APPSWE) 2576Kha: 129S6;FVB F1	Dr. Karen Ashe laboratory; Kotilinek et al.[50]	N/A
Mouse: rTg9191, FVB;129S6 F1-Tg(tetO-APPSwLon)9191Kha: FVB;129S6 F1	Liu et al.[30]; Liu et al.[2]	N/A
Mouse: 5xFAD, B6.Cg-Tg(APPSwFlLon, PSEN1*M146L*L286V)6799Vas/Mmjax: B6	Oakley et al.[36]	RRID: MMRRC_034848-JAX

(*Continued on next page*)

Continued

REAGENT or RESOURCE	SOURCE	IDENTIFIER
Mouse: APP/TTA, B6.Cg-Tg(tetO-APPSwInd) 102Dbo/Mmjax; B6	Jankowsky et al.[37]	RRID:MMRRC_034845-JAX
Mouse: FVB;129S6 F1	This paper	N/A
Software and algorithms		
GraphPad Prism version 8.3.0	GraphPad Software	RRID: SCR_002798
Image Lab version 6.1	Bio Rad	RRID: SCR_014210
Ethovision XT version 17.5	Noldus Information Technology	RRID: SCR_000441
Microsoft Excel 2016	Microsoft	RRID: SCR_016137
Optiquant version 03.00	Packard Instrument	RRID: SCR_016769
Other		
Dynabeads Protein G	Thermo Fisher Scientific	Cat#10004D
Protein G Sepharose 4 Fast Flow resin	GE healthcare	Cat#GE17-0618-02
Rabbit IgG	MilliporeSigma	Cat#I5006; RRID: AB_1163659
Neutravidin-HRP	Thermo Fisher Scientific	Cat#A2664
Streptavidin-IRDye 800CW	LI-COR Biosciences	Cat#926-32230
Superdex 200 10/300 GL column	GE healthcare	Cat#17-5175-01
BioLogic DuoFlow Chromatography system	Bio Rad	RRID: SCR_019686
ChemiDoc MP Imaging System	Bio Rad	RRID:SCR_019037

RESOURCE AVAILABILITY

Lead contact

Further information and requests for resources and reagents should be directed to and will be fulfilled by the lead contact, Karen Ashe (hsiao005@umn.edu).

Materials availability

This study did not generate new unique reagents.

Data and code availability

- All data reported in this paper will be shared by the lead contact upon request.
- This paper does not report original code.
- Any additional information required to reanalyze the data reported in this paper is available from the lead contact upon request.

EXPERIMENTAL MODEL AND STUDY PARTICIPANT DETAILS

Animals

All experiments involving mice were performed in full accordance with the guidelines of the Association for Assessment and Accreditation of Laboratory Animal Care and approved (approval #1202A09927) by the Institutional Animal Care and Use Committee at the University of Minnesota, Twin Cities, Minnesota. Mice were conventionally housed in a vivarium in which lights were on from 6 am to 6 pm (local time). Food and water were provided *ad libitum*.

To ensure the quality of cryopreservation, −80°C freezers were monitored several times a day by lab staff and were connected to carbon dioxide backup to help control significant temperature excursions in Year 2009 and prior to that. Since late Year 2009, −80°C freezers have been remotely monitored 24 h a day and 7 days a week by facilities management staff at the University of Minnesota, and we were quickly notified of any significant temperature excursions.

Vital characteristics of the transgenic animals used in this study are shown in Table S1.

Tg2576

Two-25 months Tg2576 mice[19] containing the APP_{695} isoform with the Swedish (K670N, M671L) mutation (APP-Swe) in C57B6/SJL, 129S6, or 129S6FVB background and age-matched non-transgenic littermates were from colonies in the laboratory of K.H.A. at the University of Minnesota, Twin Cities, Minnesota. Mice were anesthetized with isoflurane and sacrificed by decapitation. For each animal, the whole brain was

immediately harvested, the hemispheres were separated, and the olfactory bulb and cerebellum were then isolated from the forebrain for each hemisphere. The two hemi-forebrains, and olfactory bulb and cerebellum tissue pieces of each mouse were collected in a cryo vial, immediately snap-frozen on dry ice, and then stored at −80°C freezers until further use. Both male and female mice were used in experiments. Quantitative biochemical analyses showed no sex-related difference (Figure S30).

5xFAD

Frozen brain specimens from 9 months 5xFAD line Tg6799 mice[36] and age-matched non-transgenic littermates were kindly provided by Dr. Joanna Jankowsky at the Baylor College of Medicine, Houston, Texas. Upon receiving these frozen specimens shipped on dry ice, they were immediately transferred to and stored at −80°C until further usage. Both male and female 5xFAD mice were used. Quantitative biochemical analyses of sex-related difference were not performed due to low sample sizes.

APP/TTA

Frozen brain specimens from 10 to 11 months APP/TTA mice[37] and age-matched non-transgenic littermates were kindly provided by Dr. Joanna Jankowsky at the Baylor College of Medicine, Houston, Texas. Upon receiving these frozen specimens shipped on dry ice, they were immediately transferred to and stored at −80°C until further usage. Both male and female APP/TTA mice were used. Quantitative biochemical analyses of sex-related difference were not performed due to low sample sizes.

rTg9191

Frozen brain specimens from 24 months rTg9191 mice[30] and their age-matched non-transgenic littermates were kindly provided by Dr. George Carlson at the McLaughlin Research Institute, Great Falls, Montana. Upon receiving these frozen specimens shipped on dry ice, they were immediately transferred to and stored at −80°C until further usage. Both male and female rTg9191 mice were used. No sex-related difference in biochemical analysis was present.

Wild-type mice

FVB129S6 F1 mice were generated in house by crossing FVB females (Charles River Laboratories, Wilmington, MA; Stock# 207) with 129S6 males (Taconic Biosciences, Germantown, NY; Stock# 129SVE). For the object recognition task, we randomly assigned FVB129S6 F1 mice between 4 and 7 months of age to two different treatments. Both male and female mice were used. No sex-related difference in behavioral performance was identified. The mice were conventionally housed, maintained on a 12-h ON: 12-h OFF light cycle, and given *ad libitum* access to food and water in a vivarium.

METHOD DETAILS

Antibodies

Basic information (Table S2) and detailed usage (Table S3) of all antibodies used in this paper are shown.

Brain protein extraction

Detergent-free, aqueous brain protein extracts were prepared using a protocol adapted from a previous publication.[51] Briefly, each frozen hemi-forebrain free of olfactory bulb and cerebellum was weighed and then transferred to 5 volumes (i.e., 5 mL per g of wet brain tissue) of ice-cold extraction buffer (25 mM tris(hydroxymethyl)aminomethane-hydrochloric acid (Tris-HCl), pH 7.4; 140 mM sodium chloride (NaCl); 3 mM potassium chloride (KCl); 0.1 mM phenylmethylsulfonyl fluoride (PMSF); 0.2 mM 1,10-phenanthroline monohydrate (phen); 0.1% (v/v) protease inhibitor cocktail (MilliporeSigma, Burlington, MA); 0.1% (v/v) phosphatase inhibitor cocktail A (SantaCruz Biotechnology, Dallas, TX); and 0.1% (v/v) phosphatase inhibitor cocktail 2 (MilliporeSigma)). Each piece of brain tissue was homogenized at room temperature under the highest power for 25 strokes using a Dounce homogenizer (PolyScience, Niles, IL). The resulting material was immediately placed on ice for 5 min, then transferred into an ice-cold, sterilized, 1.5-mL microcentrifuge tube, and centrifuged at 16,100 x *g*, 4°C for 90 min. The supernatant was collected and incubated twice with 25 μL of Protein G Sepharose 4 Fast Flow resin (GE healthcare, Piscataway, NJ), each time at 4°C for 1 h, to deplete endogenous mouse immunoglobulin G (msIgG). Total protein concentrations were determined using the bicinchoninic acid (BCA) assay (Thermo Fisher Scientific, Waltham, MA). Brain protein extracts were then stored at −80°C in multiple aliquots to avoid repeated freeze-and-thaw procedures.

Size-exclusion chromatography (SEC)

SEC was performed using a Superdex 200 10/300 GL column (GE healthcare) under the control of the BioLogic DuoFlow Chromatography system (Bio-Rad, Hercules, CA).

To calibrate the column, each entity in a biomolecule standard set—eight globular proteins at the molecular weights of 669, 443, 200, 150, 66, 29, 13.4, and 6.5 kDa, and Blue Dextran, >2,000 kDa (MilliporeSigma)—was individually injected at the dose of 200 μg in 250 μL of 0.22 μm-filtered phosphate-buffered saline (PBS, pH 7.4). Biomolecule standards were eluted at room temperature with 0.22 μm-filtered PBS at a flow

rate of 0.5 mL/min and a fraction size of 250 μL. The elution chromatogram of each standard was determined by both absorbance at wavelength 280 nm and the BCA assay using a DTX880 Multimode detector (Beckman Coulter, Brea, CA).

To analyze biological samples, detergent-free, aqueous brain protein extracts of Tg2576 mice at 10–11 months of age prior to the appearance of ThioS-reactive, dense-core plaques in the forebrain[52] were pooled from 5 mice (Tables S1 and S3), each contributing 20% protein mass. The prepared sample was injected at the dose of 2 mg in 250 μL. Proteins were eluted, and the elution chromatogram was determined as described above. Immediately after the elution was complete, the microplate that collected the fractions was stored on ice. Each of the 96 fractions was transferred into a 1.5-mL sterilized microcentrifuge tube that contained 2.6 mM PMSF, 5.2 mM phen, 2.6% (v/v) protease inhibitor cocktail, 2.6% (v/v) phosphatase inhibitor cocktail A, and 2.6% (v/v) phosphatase inhibitor cocktail 2 in 10 μL of PBS. After mixing with an SEC fraction, the final concentrations of the five types of inhibitors were 0.1 mM, 0.2 mM, 0.1% (v/v), 0.1% (v/v), and 0.1% (v/v), respectively. Each inhibitor-containing fraction was evenly split into two parts, snap-frozen on dry ice, and stored at −80°C.

To confirm the reproducibility of the SEC elution profile of Aβ entities in brain extracts of Tg2576 mice at ages prior to the appearance of ThioS-reactive, dense-core plaques, detergent-free, aqueous brain protein extracts of 7–9 months Tg2576 mice were pooled (Tables S1 and S3; $N = 4$, each contributing 25% protein mass). The SEC experiments and fraction collection and preservation were performed as described above.

To compare the SEC elution of Aβ entities in brain extracts of Tg2576 mice at ages prior to versus after the appearance of ThioS-reactive, dense-core plaques, detergent-free, aqueous brain protein extracts of 15–22 months Tg2576 mice were pooled (Tables S1 and S3; $N = 8$, each contributing 12.5% protein mass). The SEC experiments and fraction collection and preservation were performed as described above.

Immunoprecipitation (IP)

IP was performed according to previously published procedures.[2] Briefly, brain extracts containing 200–400 μg of total proteins (Tables S1 and S3) were incubated with capturing reagents (Tables S1 and S3) and Protein G-coated matrix (Protein G Sepharose 4 Fast Flow resin (GE healthcare) or Dynabeads Protein G (Thermo Fisher Scientific); Tables S1 and S3) at 4°C for 14–16 h. Subsequently, the matrix was washed under a gently rotating mode (15 rpm) first in wash buffer 1 (50 mM Tris-HCl, pH 7.4; 300 mM NaCl; 1 mM ethylenediaminetetraacetic acid (EDTA); 0.1% (v/v) polyethylene glycol p-(1,1,3,3-tetramethylbutyl)-phenyl ether (Triton X-100); 0.1 mM PMSF; 0.2 mM phen; 0.1% (v/v) protease inhibitor cocktail; 0.1% (v/v) phosphatase inhibitor cocktail A; and 0.1% (v/v) phosphatase inhibitor cocktail 2) at 4°C for 5 min, and then in wash buffer 2 (50 mM Tris-HCl, pH 7.4; 150 mM NaCl; 1 mM EDTA; 0.1% (v/v) Triton X-100; 0.1 mM PMSF; 0.2 mM phen; 0.1% (v/v) protease inhibitor cocktail; 0.1% (v/v) phosphatase inhibitor cocktail A; and 0.1% (v/v) phosphatase inhibitor cocktail 2) at 4°C for 5 min.

Western blotting (WB)

WB was performed based on previously published procedures.[2,27] Detailed usage of brain protein extracts and detecting reagents are listed in Table S3.

Briefly, eluted materials from IP (Figures 1B, 2B, 4, 7B–7E, S1A, S1B, S2A, S2B, S3A, S3B, S4A, S4B, S5A, S5B, S6A, S6B, S7A, S7B, S8A, S8B, S9A, S9B, S10A, S10B, S11A, S11B, S12A, S12B, S13A, S13B, S14A, S14B, S15A, S15B, S16A, S16B, S17A, S17B, S18A, S18B, S19A, S19B, S20A, S20B, S21A, S21B, S22A, S22B, S23A, S23B, S24A, S24B, S25A, S25B, S26A, S26B, S27A, S27B, S31–S34, and S40), SEC-fractionated brain extracts (Figures 3A, 3C, S35, S36A, S36B, and S37A), immunopurified entities (Figures 5, 6A, and S38), and brain extracts (Figures 3A, 3C, S35, S36A, S36B, S37A, and S39) were electrophoretically separated by SDS-PAGE. To prepare samples for SDS-PAGE, immunoprecipitated materials (Figures 2B, 4, 7B–7E, S1A, S1B, S2A, S2B, S3A, S3B, S4A, S4B, S5A, S5B, S6A, S6B, S7A, S7B, S8A, S8B, S9A, S9B, S10A, S10B, S11A, S11B, S12A, S12B, S13A, S13B, S14A, S14B, S15A, S15B, S16A, S16B, S17A, S17B, S18A, S18B, S19A, S19B, S20A, S20B, S21A, S21B, S22A, S22B, S23A, S23B, S24A, S24B, S25A, S25B, S26A, S26B, S27A, S27B, S31, S32, S33B, S33C, S34, and S40) were eluted by agitatedly heating the matrix in 4x Laemmli sample buffer (Bio-Rad; plus 1.42 M β-mercaptoethanol) at 1,250 rpm, 95°C for 10 min. Alternatively, immunoprecipitated materials were eluted by agitatedly incubating antibody-immobilized matrix (for details, see the "antibody immobilization on dynabeads" subsection of the method details under STAR Methods) with elution buffer 3 (recipe described in the "purification of Aβ*56" subsection of the method details under STAR Methods) at 1,250 rpm, 50°C for 5 min, and the eluted materials were then treated with 4x Laemmli sample buffer at 1,250 rpm, 95°C for 5 min (Figures 1B and S33A). SEC-fractionated brain extracts (Figures 3A, 3C, S35, S36A, S36B, and S37A), immunopurified entities (Figures 5A, 5B, and 6A), or brain extracts (Figures 3A, 3C, S35, S36A, S36B, and S37A) were mixed with 4x Laemmli sample buffer plus 1.42 M β-mercaptoethanol at 1,250 rpm, 95°C for 5 min. Immunopurified entities (Figures 5C and S38) or brain extracts (Figure S39) were mixed with 4x Laemmli sample buffer without β-mercaptoethanol or heating. Electrophoresis was performed at room temperature in running buffer 1 (Cathode buffer: 100 mM Tris-HCl, pH 8.25; 100 mM tricine; and 0.1% (w/v) SDS. Anode buffer: 200 mM Tris-HCl, pH 8.9) under a constant voltage of 80 V for 150 min when using 1.0-mm-thick 10–20% Criterion Tris-tricine gels (Bio-Rad; Figures 2B, 4, S1A, S1B, S2A, S2B, S3A, S3B, S4A, S4B, S5A, S5B, S6A, S6B, S7A, S7B, S8A, S8B, S9A, S9B, S10A, S10B, S11A, S11B, S12A, S12B, S32A, S32B, S33B, S33C, and S34), in running buffer 1 under a constant voltage of 80 V for 210 min when using 1.0-mm-thick 16.5% Criterion Tris-tricine gels (Bio-Rad; Figures S13A, S13B, S14A, and S14B), in running buffer 1 under a constant voltage of 80 V for 180 min when using 1.0-mm-thick Novex 10–20% tricine gels (Thermo Fisher Scientific; Figures 1B, S15A, S15B, S16A, S16B, S17A, S17B, S18A, S18B, S19A, S19B, S20A, S20B, S21A, S21B, S22A, S22B, S23A, S23B, S24A, S24B, S25A, S25B, S26A, S26B, S27A, and S27B), or in running buffer 2 (100 mM Tris-HCl, pH 8.3; 100 mM tricine, and 0.1% (w/v) SDS) under a constant voltage of 125 V for 90 min when using 1.0-mm-thick Novex 10–20% tricine gels (Figures 3A, 3C, 5, 6A, 7B–7E, S31, S32C, S32D, S33A, S35, S36A, S36B, S37A, S38, S39, and S40).

The size-fractionated proteins were then transferred to 0.2-μm (pore size) nitrocellulose membranes (Bio-Rad) in transfer buffer 1 (25 mM Tris-HCl, 192 mM glycine, and 10% (v/v) methanol, pH not adjusted) at 4°C under a constant current of 0.4 A for 4 h when using 10–20% Criterion Tris-tricine gels (Figures 2B, 4, S1A, S1B, S2A, S2B, S3A, S3B, S4A, S4B, S5A, S5B, S6A, S6B, S7A, S7B, S8A, S8B, S9A, S9B, S10A, S10B, S11A, S11B, S12A, S12B, S32A, S32B, S33B, S33C, and S34), 16.5% Criterion Tris-tricine gels (Figures S13A, S13B, S14A, and S14B), or Novex 10–20% tricine gels (Figures 1B, 4, S15A, S15B, S16A, S16B, S17A, S17B, S18A, S18B, S19A, S19B, S20A, S20B, S21A, S21B, S22A, S22B, S23A, S23B, S24A, S24B, S25A, S25B, S26A, S26B, S27A, and S27B), or in transfer buffer 2 (25 mM Bicine, 25 mM Bis-Tris, 1 mM EDTA, pH 7.2; 0.1% (v/v) NuPAGE antioxidant (Thermo Fisher Scientific); and 10% (v/v) methanol) at room temperature or 4°C under a constant voltage of 25 V for 2 h when using Novex 10–20% tricine gels (Figures 3A, 3C, 5, 6A, 7B–7E, S31, S32C, S32D, S33A, S35, S36A, S36B, S37A, S38, S39, and S40).

In our experience, an appropriate assembly of the gel-membrane sandwich is critical for the successful detection of Aβ*56. Specifically, the interface between gel and membrane needs to be adequately moisturized with the transfer buffer; and after the membrane has been laid on top of the gel, only necessary minimal pressure should be applied to the membrane to complete the assembly. This practice avoids generating strong uneven pressure across the gel-membrane interface that may alter the contact between gel and membrane and even deform the gel. We have constantly found that failure to observe this practice led to failure in Aβ*56 detection.

Next, each protein-blotted membrane was transferred to 50 mL of PBS of room temperature, and the membrane was subjected to microwave heating under full power first for 25 s and then for 15 s with a 4-min cooling period after each episode of heating.

Following heat-induced antigen retrieval, membranes were incubated with blocking buffers at 70 rpm, room temperature for 1 h to block non-specific binding of the detecting reagents. For WB analyses using A11 antibodies (Figures 5B, 5C, and S39) and their associated secondary detection agent Neutravidin (Figure S38), blocking buffer 1 (10 mM Tris-HCl, pH 7.4; 200 mM NaCl; 0.01% (v/v) polyoxyethylene (20) sorbitan monolaurate (Tween 20); and 5% (w/v) Carnation instant non-fat dry milk powder) of room temperature was used; and for the rest WB analyses, blocking buffer 2 (10 mM Tris-HCl, pH 7.4; 200 mM NaCl; 0.1% (v/v) Tween 20; and 5% (w/v) bovine serum albumin (MilliPoreSigma)) was used.

Next, primary antibodies were added directly to the blocking buffer (see Tables S2 and S3 for the use of detecting antibodies in detail), and membranes were then incubated at 70 rpm, 4°C for 14–16 h (For Figures S35, S36B, and S38, membranes were incubated directly with the blocking buffer at 70 rpm, 4°C for 14–16 h).

Following primary antibody incubation, membranes were washed with wash buffers five times, each time at 80 rpm, room temperature for 5 min. For WB analyses using A11 antibodies (Figures 5B, 5C, and S39) as well as of Figure S38, wash buffer 3 (10 mM Tris-HCl, pH 7.4; 200 mM NaCl; and 0.01% (v/v) Tween 20) of room temperature was used; and for the rest WB analyses, wash buffer 4 (10 mM Tris-HCl, pH 7.4; 200 mM NaCl; and 0.1% (v/v) Tween 20) of room temperature was used.

For WB analyses probed with non-biotinylated primary antibodies (Figures S32A, S32B, S33B, S33C, and S39), membranes were then incubated with biotinylated Biotin-SP (long spacer) AffiniPure donkey-*anti*-rabbit IgG (H + L) (Jackson ImmunoResearch Laboratories, West Grove, PA; diluted 1:50,000 in either blocking buffer 1 of room temperature for A11 (Figure S39) or blocking buffer 2 of room temperature for D8Q7I (Figures S32A and S32B) or D3E10 (Figures S33B and S33C) at 70 rpm, room temperature for 1 h. Following the incubation with the secondary antibody, membranes were washed in wash buffers as described above. Next, membranes were first incubated with horseradish peroxidase (HRP)-conjugated Neutravidin (Neutravidin-HRP; Thermo Fisher Scientific; diluted 1:5,000 in either wash buffer 3 of room temperature (Figure S39) or wash buffer 4 of room temperature (Figures S32A, S32B, S33B, and S33C)) at 70 rpm, room temperature for 10 (Figures S32A, S32B, S33B, and S33C) or 30 (Figure S39) min, and then washed in wash buffers as described above.

For WB analyses probed with biotinylated primary antibodies (Figs. 1B, 2B, 3A, 3C, 4, 5, 6A, 7B–7E, S1A, S1B, S2A, S2B, S3A, S3B, S4A, S4B, S5A, S5B, S6A, S6B, S7A, S7B, S8A, S8B, S9A, S9B, S10A, S10B, S11A, S11B, S12A, S12B, S13A, S13B, S14A, S14B, S15A, S15B, S16A, S16B, S17A, S17B, S18A, S18B, S19A, S19B, S20A, S20B, S21A, S21B, S22A, S22B, S23A, S23B, S24A, S24B, S25A, S25B, S26A, S26B, S27A, S27B, S31, S32C, S32D, S33A, S34, S36A, S37A, and S40) or no primary antibody (Figures S35, S36B, and S38), membranes were then directly incubated with Neutravidin-HRP (diluted 1:5,000 in either wash buffer 3 of room temperature (Figures 5B and 5C for biotinylated A11; Figure S38 for Neutravidin-HRP) or wash buffer 4 of room temperature (Figures 1B, 2B, 3A, 3C, 4, 5A, 6A, 7B–7E, S7A, S7B, S8A, S8B, S9A, S9B, S11A, S11B, S13A, S13B, S14A, S14B, S15A, S15B, S16A, S16B, S17A, S17B, S18A, S18B, S19A, S19B, S20A, S20B, S21A, S21B, S22A, S22B, S23A, S23B, S24A, S24B, S25A, S25B, S26A, S26B, S27A, S27B, S31, S32C, S32D, S33A, S34, S35, S36A, S36B, S37A, and S40)) at 70 rpm, room temperature for 10 (Figures 2B, 4, S7A, S7B, S8A, S8B, S9A, S9B, S11A, S11B, and S34) or 30 (Figures 1B, 3A, 3C, 5, 6A, 7B–7E, S13A, S13B, S14A, S14B, S15A, S15B, S16A, S16B, S17A, S17B, S18A, S18B, S19A, S19B, S20A, S20B, S21A, S21B, S22A, S22B, S23A, S23B, S24A, S24B, S25A, S25B, S26A, S26B, S27A, S27B, S31, S32C, S32D, S33A, S35, S36A, S36B, S37A, S38, and S40) min, or with Streptavidin-IRDye 800CW (LI-COR Biosciences, Lincoln, NE; diluted 1:5,000 in wash buffer 4 of room temperature (Figures S1A, S1B, S2A, S2B, S3A, S3B, S4A, S4B, S5A, S5B, S6A, S6B, S10A, S10B, S12A, and S12B)) at 70 rpm, room temperature for 10 min. Next, membranes were washed wash buffers as described above.

Membranes were incubated with the SuperSignal West Femto Maximum Sensitivity Substrate (Thermo Fisher Scientific) at 200 rpm, room temperature for 5 min (Figures 1B, 2B, 3A, 3C, 4, 5, 6A, 7B–7E, S7A, S7B, S8A, S8B, S9A, S9B, S11A, S11B, S13A, S13B, S14A, S14B, S15A, S15B, S16A, S16B, S17A, S17B, S18A, S18B, S19A, S19B, S20A, S20B, S21A, S21B, S22A, S22B, S23A, S23B, S24A, S24B, S25A, S25B, S26A, S26B, S27A, S27B, S31, S32, S33, S34, S35, S36A, S36B, S37A, S38, S39, and S40). Chemiluminescence signals were developed using the Kodak Scientific Imaging film X-OMAT Blue XB (PerkinElmer Life Sciences, Waltham, MA) (Figures 2B, 4, S7A, S7B, S8A, S8B, S9A, S9B, S11A, S11B, S32A, S32B, S33B, S33C, and S34). Alternatively, signals were revealed using the ChemiDoc MP Imaging System (Bio-Rad) (Figures 1B, 3A, 3C, 5, 6A, 7B–7E, S13A, S13B, S14A, S14B, S15A, S15B, S16A, S16B, S17A, S17B, S18A, S18B, S19A, S19B, S20A, S20B, S21A, S21B, S22A,

S22B, S23A, S23B, S24A, S24B, S25A, S25B, S26A, S26B, S27A, S27B, S31, S32C, S32D, S33A, S35, S36A, S36B, S37A, S38, S39, and S40). For membranes incubated with Streptavidin-IRDye 800CW, signals were revealed using an LI-COR Model 9120 Odyssey Infrared Imaging System (LI-COR Biosciences) (Figures S1A, S1B, S2A, S2B, S3A, S3B, S4A, S4B, S5A, S5B, S6A, S6B, S10A, S10B, S12A, and S12B). Densitometry-based quantification of protein band intensities was performed using either Optiquant version 03.00 (Packard Instrument, Fallbrook, CA) (Figures S1 and S27) or Image Lab version 6.1 (Bio-Rad) (Figures 3, 6A, S36, and S37).

To determine whether the ~56-kDa, Aβ-containing entity was present in each studied Tg2576 and rTg9191 mice, the band total intensity (i.e., the product of mean intensity per pixel and numbers of pixels in the designated band area) of the ~56-kDa, Aβ-containing entity was first measured. Next, the mean and standard deviation (SD) of background intensities were determined from the measured total intensities of four areas, each of which had an equal size to the size of the designated band area of the ~56-kDa, Aβ-containing entity. The four areas were sampled at 1) the ~56-kDa in the lane containing immunoprecipitated entities from non-transgenic mice, 2) the ~4.5-kDa (corresponding to the migrating area of monomeric Aβ) in the lane containing immunoprecipitated entities from non-transgenic mice, 3) the ~56-kDa in the lane containing only capturing antibodies but no immunoprecipitated entities from mice, and 4) the ~4.5-kDa in the lane containing only capturing antibodies but no immunoprecipitated entities from mice. The ~56-kDa, Aβ-containing entity was considered detected (i.e., present) in the brain of an animal if its band total intensity is equal to or higher than three SDs above the mean background intensity.

The experimental settings for each (IP)/WB reaction are shown in Table S3. The original WB images, the illustration of the quantification of the ~56 kDa entity, and the quantification results are shown in Figures S1 and S27.

Denaturant treatment

Three hundred and seventy-five μg of mouse brain extracts (Tables S1 and S3) were completely dried but not over-dried at room temperature using a speed vacuum concentrator (Eppendorf, Hamburg, Germany). The resulting materials were first gently and fully resuspended in 70 μL of 8 M urea (in 20 mM Tris-HCl, pH 8.0), 6 M GuHCl (in 20 mM Tris-HCl, pH 8.0), 100% (v/v) HFIP, or TBS (50 mM Tris-HCl, pH 7.4; and 150 mM NaCl; serving as a positive control for the detection of the ~56-kDa, Aβ-containing entity), and then agitated at 4°C, 1,200 rpm for 16–18 h. Brain extracts of age-matched, non-transgenic mice similarly treated with TBS served as a negative control for the detection of the ~56-kDa, Aβ-containing entity. Following the treatments, the samples were dried using the speed vacuum concentrator at room temperature for 15 min to evaporate the solvents, 1.4 mL of TBS (containing 0.1 mM PMSF, 0.2 mM phen, 0.1% (v/v) protease inhibitor cocktail, 0.1% (v/v) phosphatase inhibitor cocktail A, and 0.1% (v/v) phosphatase inhibitor cocktail 2) was added to each sample, and the samples were gently resuspended until they were fully homogenized. The resulting materials were subjected to IP as described in the "immunoprecipitation (IP)" subsection of the method details under STAR Methods.

Antibody immobilization on Dynabeads

The antibody immobilization was carried out as previously described.[49,53] Briefly, 62 μg of the D8Q7I or D3E10 antibody was incubated in 1 mL of TBS with Dynabeads Protein G matrix from 1 mL of fully resuspended slurry (settled bead volume: ~100 μL) under a gently rotating mode (15 rpm) at 4°C for 14–16 h. The antibody was covalently linked to the matrix by incubating with 1 mL of 70 mM dimethyl pimelimidate (Thermo Fisher Scientific; dissolved in triethanolamine buffer solution (MilliporeSigma) that contains 200 mM triethanolamine and pH adjusted to 9.0) solution under a gently rotating mode (15 rpm) at room temperature for 15 min. The crosslinking reaction was then quenched by incubating the antibody-matrix complex with 1 mL of 10% (v/v) ethanolamine (MilliporeSigma; diluted 100% (v/v) stock solution 10-fold in distilled deionized water) solution under a gently rotating mode (15 rpm) at room temperature for 15 min. Prior to use, beads were pre-treated twice with elution buffer 1 (100 mM glycine-HCl, pH 2.9; and 1 M urea) under a gently rotating mode (15 rpm) at room temperature for 5 min to wash off any antibody not covalently linked to beads. The antibody-matrix complex was stored at 4°C in TBS containing 0.05% (w/v) sodium azide and inhibitors (0.1 mM PMSF, 0.2 mM phen, 0.1% (v/v) protease inhibitor cocktail, 0.1% (v/v) phosphatase inhibitor cocktail A, and 0.1% (v/v) phosphatase inhibitor cocktail 2).

Immunoaffinity purification

Brain protein extracts (Tables S1 and S3) of 15–22 months Tg2576 or age-matched non-transgenic mice were incubated with D8Q7I-bound Dynabeads Protein G matrix (Table S3) under a gently rotating mode (15 rpm) at 4°C for 20 h. The immunocomplex-matrix was then washed twice with 1 mL of wash buffer 5 (TBS plus 1% (w/v) *n*-Octyl *β*-D-thioglucopyranoside (OTG)) under a gently rotating mode (15 rpm) at 4°C for 5 min. Immunoprecipitated entities were eluted three times using 50 μL of elution buffer 2 (Pierce IgG Elution Buffer, pH ~3 (Thermo Fisher Scientific); and 1% (w/v) OTG) by agitating at 1,200 rpm, 25°C for 5 min. Each time immediately after the elution, the pH of the eluted material was neutralized to pH between 7 and 8 using a neutralization solution (1 M Tris-base (pH ~10.5)). The eluted materials were stored at −80°C.

Purification of Aβ*56

We used immunoaffinity purification coupled to SDS-PAGE/electro-elution to purify Aβ*56 from Tg2576 mouse brains.

Immunoaffinity purification, as described in the "immunoaffinity purification" subsection of the method details under STAR Methods, was performed by incubating brain extracts (3 mg total proteins) of Tg2576 mice (Tables S1 and S3) with D8Q7I (31 μg)-bound Dynabeads Protein G matrix (0.5 mL) (Table S3). To enhance the elution efficiency, we eluted immunoprecipitated entities using 100 μL of elution buffer 3 (Pierce IgG Elution Buffer, pH ~3; 1% (w/v) OTG; and 2 M urea). The matrix was agitated at 1,200 rpm, 50°C for 5 min each time, and the elution was performed twice. Immediately following the elution step, 1) the eluted materials were combined, neutralized to pH between 7 and 8 using the

neutralization solution, and stored at −80°C; and 2) the D8Q7I-bound Dynabeads Protein G matrix was neutralized using TBS and stored at 4°C (for long-term storage, including 0.05% (w/v) sodium azide). Compared to the elution using elution buffer 2 at room temperature, the additional 2 M urea in elution buffer 3 and the adjustment of the elution temperature to 50°C increased the yield of Aβ*56 by nearly 5- and more than 30–fold, respectively.

To further isolate Aβ*56 from other Aβ entities, the eluted materials were size-fractionated by SDS-PAGE under denaturing conditions using 1.0-mm-thick Novex 10–20% tricine gels. Ten percent of the fractionated proteins were then subjected to WB using the protocol described in the "western blotting (WB)" subsection of the method details under STAR Methods that was used to generate Figure 5A. After WB, the rest of the gel piece in which the other 90% of eluted materials were fractionated was overlaid on the WB image using protein molecular weight standards for alignment. The locations of Aβ*56 were identified, and the gel pieces containing Aβ*56 were excised and subjected to electro-elution.

Aβ*56 was eluted from the gel pieces using a Bio-Rad Model 422 Electro-eluter (Bio-Rad) following the manufacturer's instructions. Electro-elution was carried out in elution buffer 4 (50 mM ammonium bicarbonate, pH 8.8; and 0.1% (w/v) SDS) at room temperature under a constant current of 10 mA for 6 h with the buffer being changed once after 3 h. At the end of the electro-elution, the polarity of the electrodes was reversed; the electro-elution was then carried out at room temperature under a constant current of 10 mA for 1 min to remove proteins from the dialysis membrane.

The sample collected from electro-elution was then subjected to detergent removal at room temperature for three times using High Protein and Peptide Recovery Detergent Removal Resin (Thermo Fisher Scientific) following the manufacturer's instructions. Using a spectroscopic assay,[54] the SDS concentration after the detergent removal step was determined to be <0.01% (w/v), which was more than 20-fold below the critical micelle concentration of SDS in water at room temperature. Finally, the storage buffer of the sample was switched to PBS using Amicon filters (MilliporeSigma; MWCO = 10 kDa) following the manufacturer's instructions. The final product was stored at −80°C.

The yields of Aβ*56 in the process of purification were estimated using densitometry-based quantification of WB probed with the 82E1 antibody. Synthetic Aβ(1–40) standards of known concentrations were used to establish a linear relationship (standard curve with an equation) between protein mass and band intensity. The concentrations of Aβ*56 were estimated by fitting their band intensity values to the standard curve. Here, we assumed that the binding stoichiometry of 82E1 and the monomeric Aβ(1–40) standards is equal to that of 82E1 and Aβ*56 (i.e., 1:1) and that Aβ*56 is composed of 12 monomeric Aβ(1–40). We estimated that the yields of Aβ*56 isolated from 17 to 22 months Tg2576 mice at the completion of immunoaffinity purification, electro-elution, and detergent removal/PBS buffer exchange steps were ∼2,880 ng, ∼960 ng, and ∼480 ng per g wet forebrain mass, respectively (forebrain is defined as whole brain ridding olfactory bulb and cerebellum; 1 g wet forebrain mass contains ∼30 mg water-soluble proteins).

Silver stain

The purity of isolated Aβ*56 was assessed by silver stain using a SilverQuest Silver Staining Kit (Thermo Fisher Scientific) following the manufacturer's instruction. Purified Aβ*56, stored in PBS, was denatured in denaturing conditions and then subjected to SDS-PAGE using a 1.0-mm-thick Novex 10–20% tricine gel. The stained gel was scanned using an Epson Perfection V100 PHOTO Flatbed Scanner (Epson America, Los Alamitos, CA) to obtain images.

Object recognition test (ORT)

Mice

We used male and female FVB129S6 F1 mice between 4 and 7 months of age. The mice were conventionally housed at room temperature in a vivarium in which lights were on from 6 am to 6 pm (local time). Food and water were provided *ad libitum*. Mouse behavioral tests were performed at room temperature.

Testing arena

The arena consisted of a round steel basin (Behrens, Excelsior, MN), 50 cm in diameter and 28 cm in height, the interior of which was painted khaki (Rust-Oleum Camouflage Spray Paint). The bottom of the basin was covered with approximately 0.25 cm of fresh, sanitized corncob bedding (Teklad, Madison, WI) mixed with a handful of bedding from the cages of each animal to be tested on a given day. Urine and feces were removed after each test. The bedding was changed between testing days.

Testing room

Animals were tested in a 2.74 m × 3.66 m rectangular room with a table in the center on which the testing arena was placed. Lamps were placed approximately 80 cm to the left and right of the table, and an overhead light was adjusted to illuminate the testing arena at an intensity of 60 lux. A video camera was mounted over the table. The tester sat by a computer in a corner of the room out-of-sight of the mice.

Test objects

The familiar object was a T25 culture flask filled with non-toxic white powder with red dots on each side, and the novel object was a Lego tower. They were placed opposite to each other 8 cm from the rim of the basin. Both the Lego tower and T25 flask were 10 cm tall and 5 cm wide.

Procedure

Mice commenced the ORT 23 h after receiving injections. They were not pre-handled, but were habituated to the testing room 30 min before the training trial. ***Training trial***: Mice explored two identical culture flasks for a total of 30 s. A mouse was excluded as it did not meet the 30-s criterion in 8 min. Mice were returned to their home cages after the trial. ***Inter-trial interval***: 3 h. ***Testing trial***: Mice explored a third copy of the culture flask along with the Lego tower for a total of 30 s. Lego tower location was randomized to control for a place preference across gender, treatment, and time of day. All testing was performed between 6:30 am and 3:30 pm (local time). Personnel were blind to treatment groups throughout the entire ORT test.

Analysis

We used Ethovision XT (version 17.5) (Noldus Information Technology, Leesburg, VA) to capture and track videos and for data analysis. Exploration time was defined as the mouse maintaining its nose within a 2-cm boundary zone around an object. Body contour was detected using dynamic subtraction with extra correction of nose-tail swaps enabled. Tracking automatically terminated after accumulating 30 s of total exploration time, or after a maximum of 8 min. We used the Excel Analysis ToolPak (Microsoft Corporation, Redmond, WA) to perform statistical calculations and GraphPad Prism (version 8.3.0) (GraphPad Software, La Jolla, CA) to create graphs. We found no main-effect of sex and included both sexes in the analysis.

Aβ*56 injection into brains of wild-type mice

Four to 7-month-old naive FVB129F1 mice received injections of Aβ*56 or PBS in the left and right hippocampi 23 h prior to the training phase of the ORT. Mice were anesthetized with isoflurane, USP (Dechra Pharmaceuticals, Fort Worth, TX). Burr holes were made at coordinates −2.3 mm (Antero-Posterior) and +/−2.0 mm (Medio-Lateral). Half a μL of Aβ*56 (3.9 ng/μL) or PBS were injected into each side (at −1.6 mm DorsoVentral) using a 1701SN (10 μL, 33 GA) Hamilton syringe connected to a UMP-3 autoinjector (World Precision Instruments, Sarasota, FL) automatic injector over 5 min. All injections were performed between 6:30 am and 1:30 pm (local time). Injections of Aβ*56 or PBS were distributed to control for gender and time of day. Mice were singly housed after surgery. Personnel performing surgical injections were blind to treatment groups.

QUANTIFICATION AND STATISTICAL ANALYSIS

To determine whether a ~56-kDa, SDS-stable, water-soluble, Aβ(x-40)-containing entity is present in aqueous forebrain extracts of individual Tg2576 and rTg9191 mice (Figures 1C and S1–S27; Tables S1 and S3), descriptive statistical comparisons were performed. A total of $N = 171$ male and female Tg2576 mice between 2 and 25 months of age, a total of $N = 38$ age- and sex-matched non-transgenic littermates of Tg2576 mice, a total of $N = 6$ male and female rTg9191 mice at 24 months of age, and a total of $N = 2$ age- and sex-matched non-transgenic littermates of rTg9191 mice were randomly chosen from the frozen brain tissue bank in the laboratory of K.H.A. at the University of Minnesota, Twin Cities, Minnesota. Protein band intensities were measured using a densitometry-based approach. That intensities of the ~56-kDa entities of individual transgenic mice that were equal or higher than three SDs above the mean background intensity was the criterion used to determine the presence of the measured molecules. Detailed statistical analyses were described in the "western blotting (WB)" subsection of the method details under STAR Methods and illustrated in Figures S1 and S27. When calculating the percent mice with the ~56-kDa entities (Figure 1C), we stratified the data of Tg2576 mice into four age groups in a way to assure a decent sample size ($N \geq 12$) within each group.

To determine in each measured SEC fraction the relative levels of Aβ entities in aqueous brain extracts of Tg2576 mice (Figures 3B, 3D, S36C, and S37B), descriptive statistical analyses were performed. Brain extracts of Tg2576 mice at three different ages were pooled from $N = 5$ (Figures 3B and 3D), $N = 4$ (Figure S36C), and $N = 8$ (Figure S37B) were used. Densitometry-based protein band intensities were measured and normalized intensities of Aβ entities of interest in each measured SEC fraction were plotted. Detailed statistical analyses were described in the "size-exclusion chromatography (SEC)" subsection of the method details under STAR Methods and legends of Figures 3, S36, and S37.

To compare levels of the ~56-kDa Aβ entities in Tg2576 mice of different ages (Figure S28), we measured their levels of in a subgroup ($N = 35$) of 6–25 months mice. The ID list of the selected animals is shown in the legend of Figure S28. Due to variations in experimental settings, such as images collected using different media (film versus digital images) and WB performed with different types of acrylamide gels, we were unable to use the entire dataset to explore the relationship between age and the ~56 kDa Aβ entity level. This subgroup was selected because the WB images of Aβ entities in these animals were collected under the same experimental settings. We categorized the ages into three groups, 6–11 months ($N = 11$), 12–17 months ($N = 10$), and 20–25 months ($N = 14$) so that they are in consistent with the age periods shown in Figure 1C. In addition, each group has a decent sample size ($N \geq 12$). For statistical analyses, levels of the~56-kDa Aβ entities of each age group were first subjected to the D'Agostino & Pearson test, Anderson-Darling test, Shapiro-Wilk test, and Kolmogorov-Smirnov test, respectively, to examine whether the data fit the normal distribution. None of the four tests showed that all three sets of data were normally distributed; therefore, the non-parametric Kruskal-Wallis test was used to compare protein levels between the three groups. *Post hoc* analyses between each two of the three groups were carried out using the Dunn's multiple comparisons test. Data of individual mice plus group median ± interquartile range and p values of *Post hoc* analyses indicating significant differences were illustrated in Figure S28. A p value of less than 0.05 was considered statistically significant. Detailed statistical analyses results were described in the results section and the legend of Figure S28.

To determine the correlation between levels of the ~56-kDa Aβ entities and Aβ(1–40) monomers in Tg2576 mice (Figure S29), we measured their levels of in a subgroup (N = 35) of 6–25 months mice. The ID list of the selected animals is shown in the legend of Figure S29. The rationale behind sample selection was described above. For statistical analyses, levels of the~56-kDa Aβ entities of the N = 35 mice and levels of Aβ(1–40) monomers of the N = 35 mice were separately subjected to the D'Agostino & Pearson test, Anderson-Darling test, Shapiro-Wilk test, and Kolmogorov-Smirnov test, respectively, to examine whether the data fit the normal distribution. All four tests showed that neither datasets were normally distributed; therefore, the non-parametric Spearman rank-order correlation was used. A scatterplot illustrating data of individual mice, the correlation coefficient, and two-tailed p value were shown in Figure S29. A p value of less than 0.05 was considered statistically significant. Detailed statistical analyses results were described in the results section and the legend of Figure S29.

To compare the levels of the ~56-kDa Aβ entities between male and female Tg2576 mice (Figure S30), we measured their levels of in a subgroup (N = 35) of 6–25 months mice. The ID list of the selected animals is shown in the legend of Figure S30. The rationale behind sample selection was described above. For statistical analyses, levels of the~56-kDa Aβ entities of the N = 19 male and N = 16 female mice were separately subjected to the D'Agostino & Pearson test, Anderson-Darling test, Shapiro-Wilk test, and Kolmogorov-Smirnov test, respectively, to examine whether the data fit the normal distribution. None of the four tests showed that both datasets were normally distributed; therefore, the non-parametric two-tailed Mann-Whitney U test was used. Data of individual mice plus group median ± interquartile range and the p value were illustrated in Figure S30. A p value of less than 0.05 was considered statistically significant. Detailed statistical analyses results were described in the results section and the legend of Figure S30.

For densitometry-based quantification of Aβ*56 (Figure 6B), the band intensities of synthetic Aβ(1–40) of known concentrations were fit using linear regression (the least squares method) whiling the generated straight line was forced through point (x = 0, y = 0). Data of individual band intensities, and the fit linear curve, generated equation, goodness of fit (an R^2 value) were shown in Figure 6B.

To assess the ORT performance of mice in response to Aβ*56 administration (Figure 6E), both male and female mice were used, which is supported by preliminary data showing no sex-related difference in ORT performance. Wild-type 129S6FVBF1 mice of 4–7 months of age were randomly chosen for surgical injections and subsequent behavioral tests. Mice that did not meet the 30-s exploration criterion in 8 min during the training trials were excluded. Sample size estimation was carried out based on preliminary ORT data of mice injected with Aβ*56 or PBS vehicle: For a mean difference in DI values of 0.12, a common SD of DI values of 0.09, a group size of N = 3, and a Type I error rate (α) of 0.05, we estimated that a sample size of N = 9 was required to gain a statistical power (1-β) of 0.80. For statistical analyses, the DI values of Aβ*56-treated mice (N = 8) and those of vehicle-treated mice (N = 13) were separately subjected to the D'Agostino & Pearson test, Anderson-Darling test, Shapiro-Wilk test, and Kolmogorov-Smirnov test, respectively, to examine whether the data fit the normal distribution. All four tests showed that both datasets were normally distributed. Both the parametric, two-tailed, unpaired t-test with Welch's correction ($t_{18.91}$ = 2.711, p = 0.0139) and the non-parametric, two-tailed, unpaired Mann-Whitney U test were used for comparison. Data of individual mice plus group median ± interquartile range and the p value were shown in Figure 6E. A p value of less than 0.05 was considered statistically significant. Detailed statistical analyses results were described in the results section and the legend of Figure 6E.

All statistical analyses were performed using Microsoft Excel 2016 and GraphPad Prism (version 8.3.0).